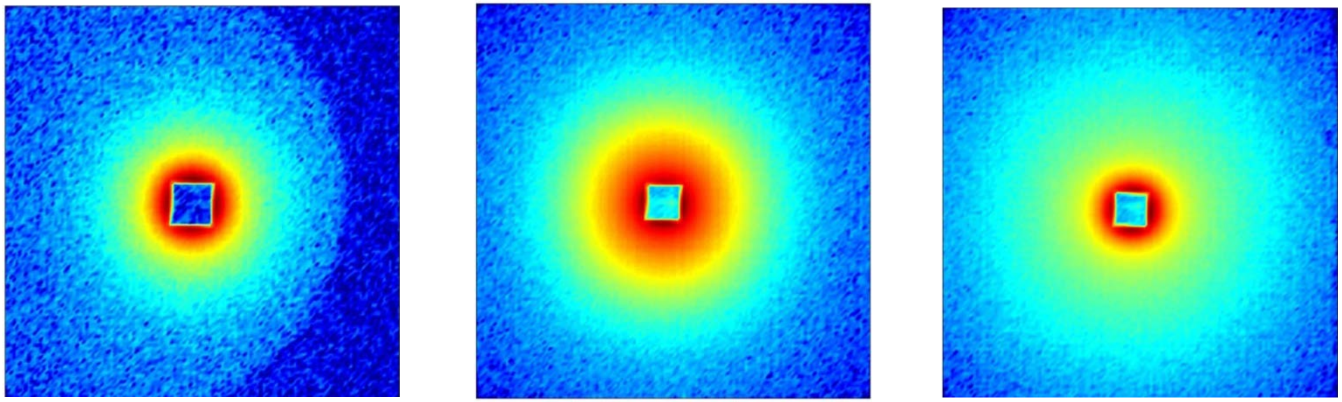

Small Angle Scattering on Metals with Neutrons and X-rays

Niels van Dijk

Fundamental Aspects of Materials and Energy, TU Delft

3-6-2015

n.h.vandijk@tudelft.nl

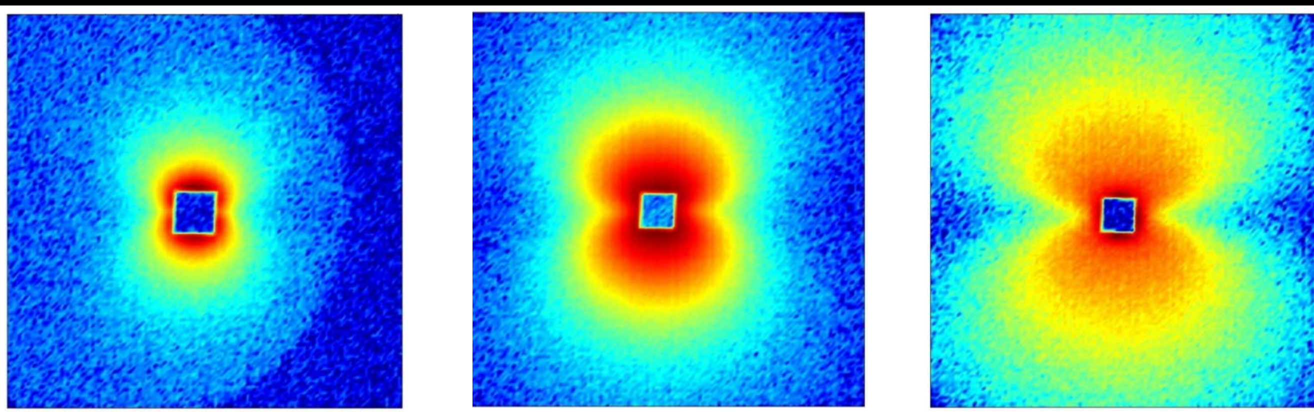

Outline

- Introduction:
    - Nanoscale structures in metals
- Experimental Methods:
    - Summary SAS
    - When to use SAS
    - Comparison SANS & SAXS
- Examples:
    - SANS on precipitates
    - SAXS on precipitates
    - Small-angle diffraction with SANS

Improved functionality by nanostructuring materials

Precipitation hardening Al-Cu (4 at.%)

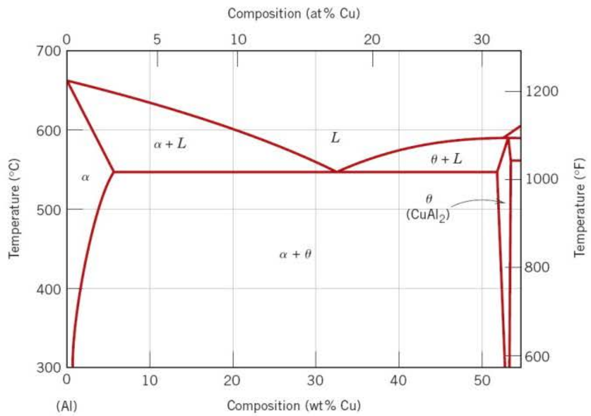

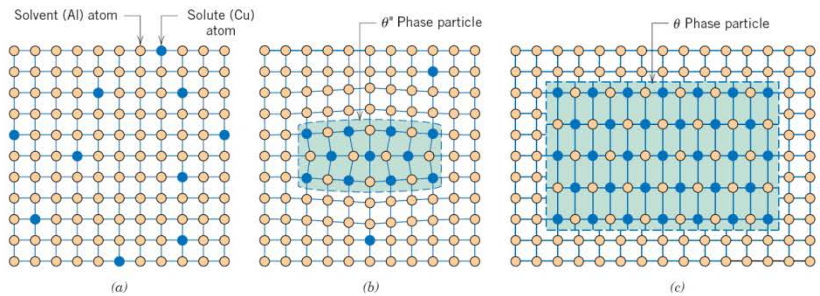

Figure 11.25 Schematic depiction of several stages in the formation of the equilibrium precipitate (θ) phase. (*a*) A supersaturated α solid solution. (*b*) A transition, θ'', precipitate phase. (*c*) The equilibrium θ phase, within the α-matrix phase.

precipitation

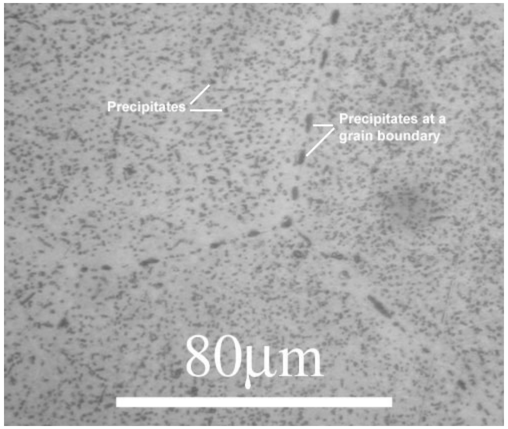

Strength during aging

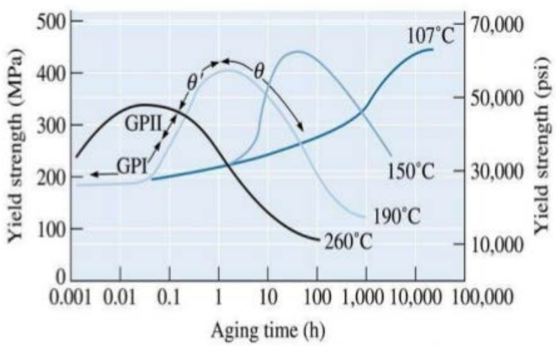

Murray,
Int. Metals Rev. 30 (1985) 5.

Structure evolution during phase transformations in structural materials

Nucleation: formation of new phase particles

- nm size clusters
- occurs on short time scales
- positioned within bulk materials
- strongly dependent on interface/defect properties

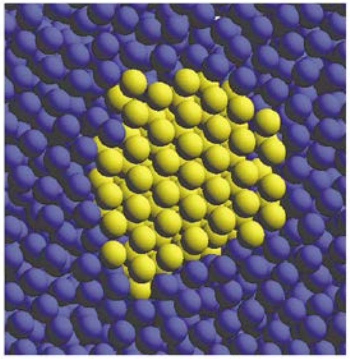

Nucleus hard-sphere colloid

Growth: increase in size of nucleated grain

- controlled by diffusion of alloying elements and/or heat
- interaction between neighboring growing particles
- dependent on microstructure of the parent phase

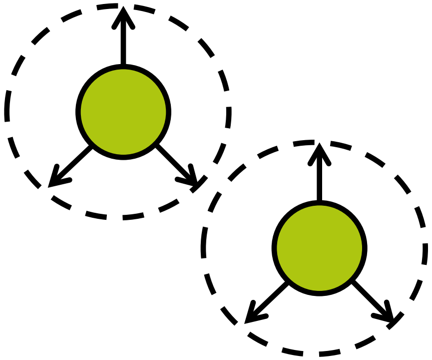

→ Need for time-dependent in-situ measurements

Nanoscale probes

Small-Angle X-ray Scattering

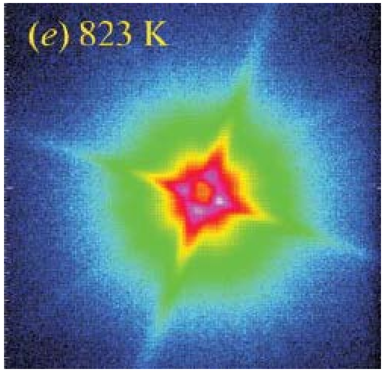

Small-Angle Neutron Scattering

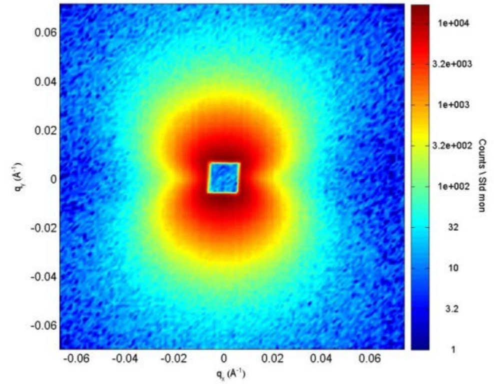

Transmission Electron Microscopy

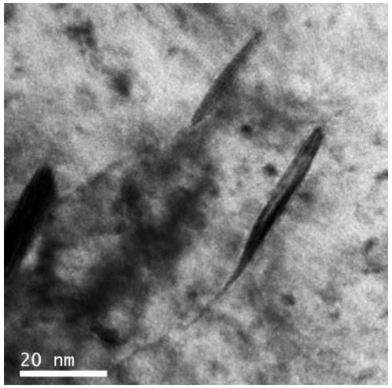

Atom probe Tomography

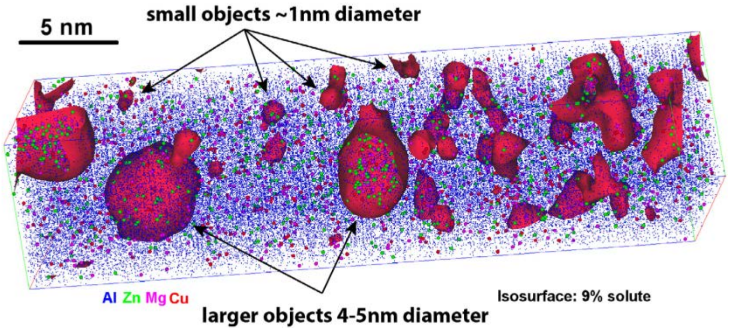

Hutchinson *et al.*, Acta Materialia 74 (2014) 96.

Nanoscale probes

Small-Angle X-ray Scattering
+ Non destructive
+ In situ / time resolved
+ Contrast near absorption edge
+ High flux
- Sample thickness heavy elements
- No spatial information
- Indirect chemical information

Small-Angle Neutron Scattering
+ Non destructive
+ In situ / time resolved
+ Magnetic information
+ Can probe a large volume
- Flux limited
- No spatial information
- Indirect chemical information

Transmission Electron Microscopy
+ Up to atomic spatial resolution
+ Can provide chemical information
- Destructive
- Probes limited volume

Atom probe Tomography
+ Near atomic spatial resolution
+ Precise chemical information
- Destructive
- Probes limited volume

Combining techniques will provide complementary information

Small Angle Scattering:
Elastic Scattering

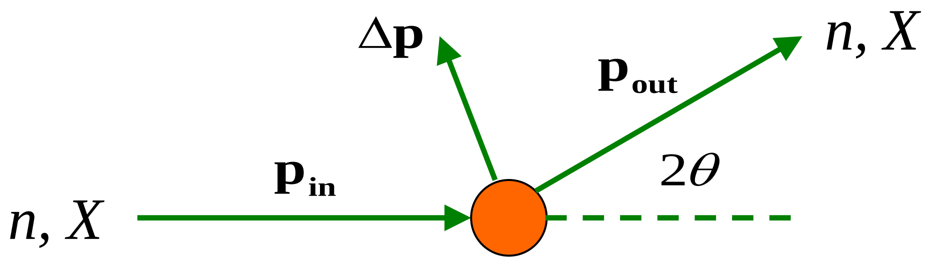

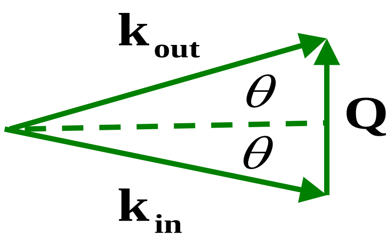

Momentum conservation:

$$\mathbf{p}_{\text{out}} = \mathbf{p}_{\text{in}} + \Delta\mathbf{p}$$

$$\hbar\mathbf{k}_{\text{out}} = \hbar\mathbf{k}_{\text{in}} + \hbar\mathbf{Q}$$

$$\boxed{\mathbf{Q} = \mathbf{k}_{\text{out}} - \mathbf{k}_{\text{in}}}$$

Energy conservation:

$$E_{\text{out}} = E_{\text{in}} + \cancel{\Delta E} = E_{\text{in}}$$

Neutrons: $\dfrac{|\mathbf{p}_{\text{out}}|^2}{2m} = \dfrac{|\mathbf{p}_{\text{in}}|^2}{2m} \rightarrow |\mathbf{p}_{\text{out}}| = |\mathbf{p}_{\text{in}}|$

X-rays: $c|\mathbf{p}_{\text{out}}| = c|\mathbf{p}_{\text{in}}| \rightarrow |\mathbf{p}_{\text{out}}| = |\mathbf{p}_{\text{in}}|$

$$\boxed{|\mathbf{k}_{\text{out}}| = |\mathbf{k}_{\text{in}}| = k = \frac{2\pi}{\lambda}}$$

$\mathbf{k}$ = wave vector
$\mathbf{Q}$ = wave vector transfer
λ = wavelength
2θ = scattering angle

Wave vector transfer : $\boxed{Q = \dfrac{4\pi}{\lambda}\sin(\theta)}$

Interference pattern: $I(\mathbf{Q}) \propto |f(\mathbf{Q})|^2$

Fourier transform of object $f(\mathbf{Q}) = \int \rho(\mathbf{r}) e^{i\mathbf{Q}\cdot\mathbf{r}} d^3\mathbf{r}$

sphere

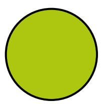

$|f(\mathbf{Q})|^2$

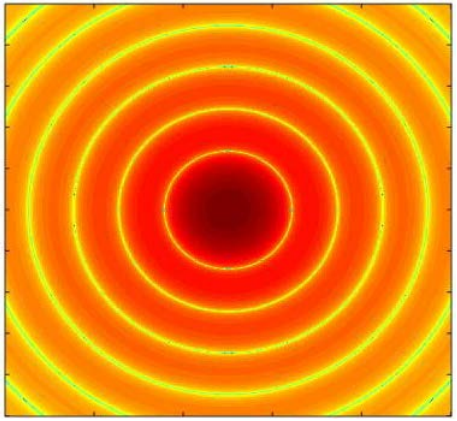

cube

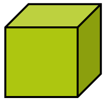

$|f(\mathbf{Q})|^2$

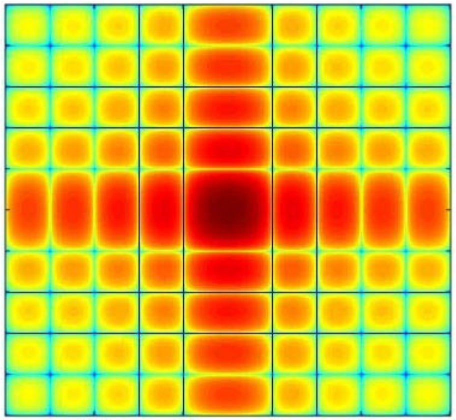

block

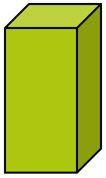

$|f(\mathbf{Q})|^2$

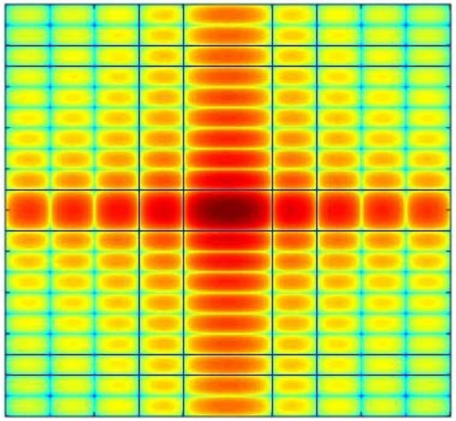

Note: patterns are in log scale

Scattered Intensity:

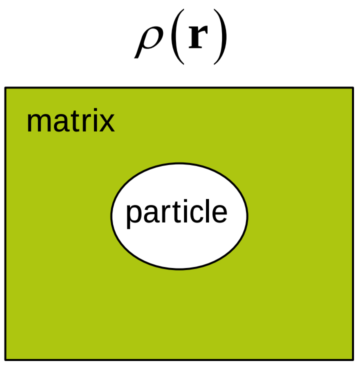

$$\boxed{\left(\frac{d\Sigma}{d\Omega}\right)(Q) = (\Delta\rho)^2 \int_0^\infty D_N(R) V^2(R) P(Q,R)\, dR}$$

Contrast : $(\Delta\rho)^2 = \left(\rho_{particle} - \rho_{matrix}\right)^2$

Orientation - averaged square of formfactor : $P(Q,R) = \int_0^{\pi/2} |f|^2 \sin(\alpha)\, d\alpha$

Particle volume : $V(R)$

Number distribution of size particles : $D_N(R)$

Assumptions :

1. dilute limit (low volume fraction of particles within the matrix)
2. weak scattering (<10% of the X-rays or neutrons are scattered)

Contrast X-rays:

$\rho(\mathbf{r})$

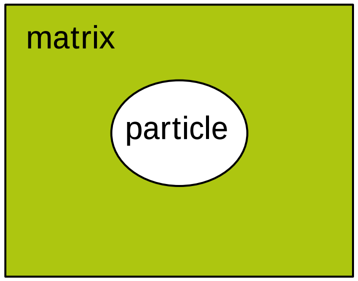

$$\boxed{(\Delta\rho)^2 = \left(\rho_{particle} - \rho_{matrix}\right)^2}$$

Sensitive to variations in:

- Chemical composition
- Density

Contrast Neutrons:

$\rho(\mathbf{r})$

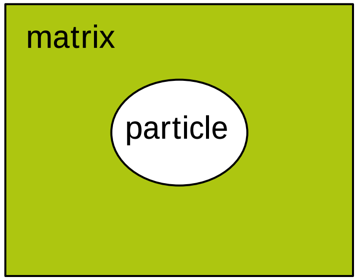

Nuclear contrast:

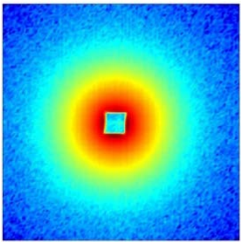

$$\boxed{(\Delta\rho)^2 = \left(\rho_{particle} - \rho_{matrix}\right)^2}$$ with $$\boxed{\rho = \sum_i N_0^{\,i} b_c^{\,i}}$$

N_0 = number density
b_c = scattering length
ρ = scattering length density

Sensitive to variations in:

- Chemical composition
- Density

Magnetic contrast:

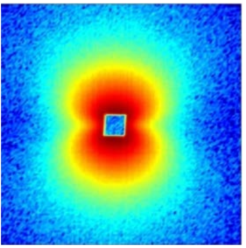

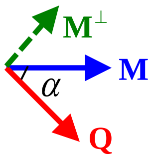

$$\boxed{(\Delta\rho)^2 = p_0^{\,2}\left(M^{\perp}{}_{particle} - M^{\perp}{}_{matrix}\right)^2 = p_0^{\,2}\left(M_{particle} - M_{matrix}\right)^2 \sin^2\alpha}$$ with $$\boxed{M = \sum_i N_0^{\,i} \mu^i}$$

N_0 = number density
μ = magnetic moment
M= magnetisation

Sensitive to variations in:

- Size magnetic moment
- Density
- Orientation magnetic moment

Considerations SAXS on metals

Anomalous SAXS:

Close to an absorption edge X-ray scattering depends on the energy:

$$f = f^{0}(\mathbf{Q}) + f'(E) + if''(E)$$

This gives additional contrast and can provide additional chemical information.

Sample transmission:

The transmission X-rays with E<30 keV leads to restrictions in the allowed sample thickness (especially for heavy elements).

Additional scattering for crystalline materials (metals):

X-rays with 10-30 keV have a wavelength of λ = 0.4-1.2 Å.
This allows for a possible diffraction signal.

Considerations SANS on metals

Magnetic SANS:
For magnetic materials the particles have both nuclear and magnetic contrast that probe the sample particle size distribution. The ratio between them may provide chemical information.

Contrast:
As the coherent scattering length strongly varies from element to element the contrast strongly depends on the composition.

Sample transmission:
The large penetrating power of neutrons generally allow a large sample thickness (and sample volume to be probed).

No additional diffraction signal:
In SANS neutrons have a wavelength of λ = 6-10 Å.
This generally does not allow Bragg scattering.

Data analysis

Data reduction:

Transform the raw intensity data on the 2D detector $I(x,y)$ into instrument independent 1D SAS data of $(d\Sigma/d\Omega)(Q)$ versus Q.

Model fitting: (SASfit, Grasp, GNOM, ...)

Construct a model of the scattering objects and obtain the relevant model parameters by fitting.
Additional information from other methods (TEM, Atom probe) is generally very useful to obtain reliable results.

Example:

SANS on Cu precipitation in deformed Fe-Cu alloys

Scattering from inhomogeneities

1. Nuclear contrast: scattering length density ρ

$$\Delta\rho^2 = (\underset{\text{particle}}{\rho_p} - \underset{\text{matrix}}{\rho_m})^2$$

2. Magnetic contrast: magnetisation $\mathbf{M}$

$$\Delta M^2 = (\underset{\text{particle}}{M_p} - \underset{\text{matrix}}{M_m})^2$$

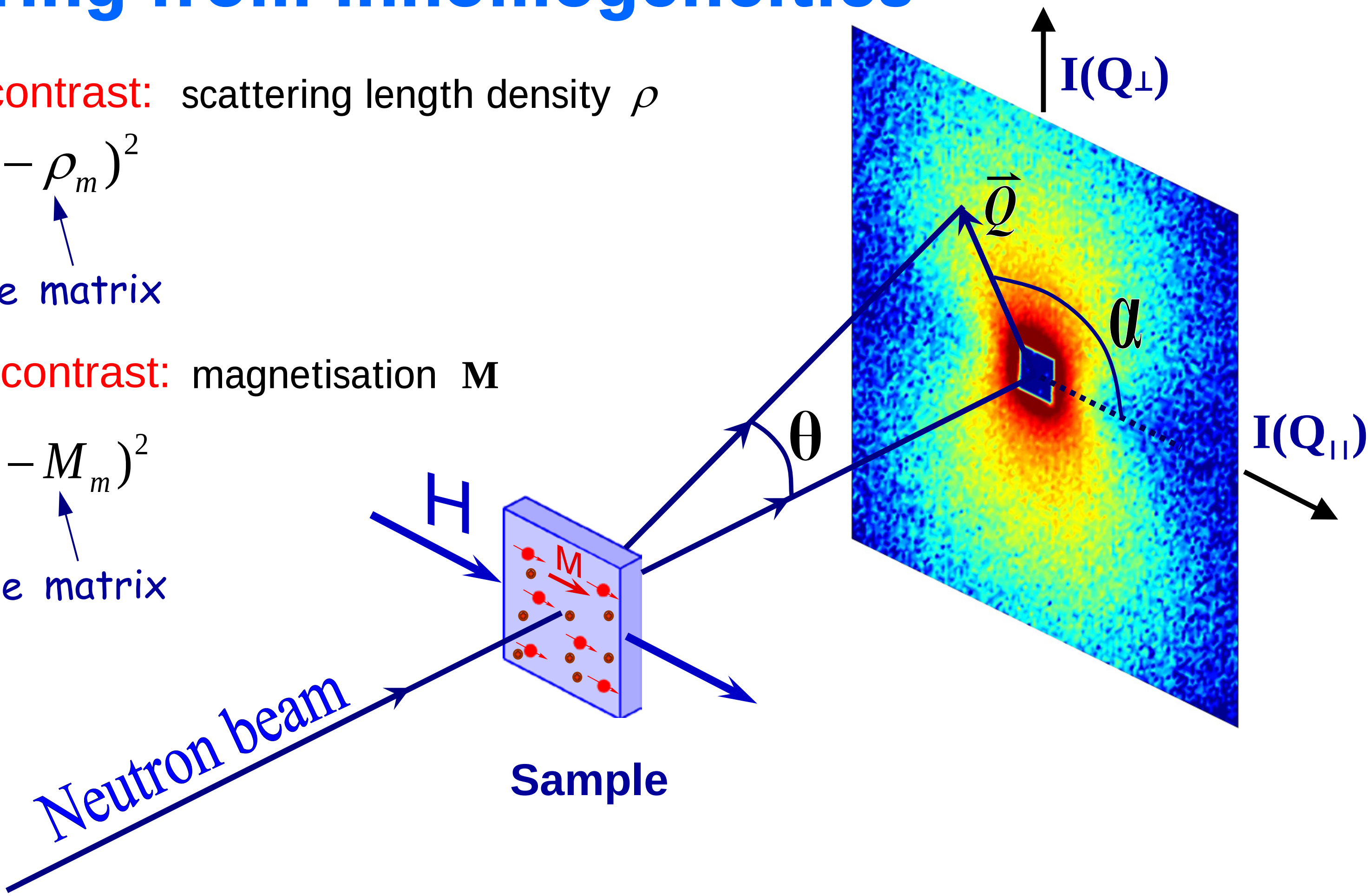

Neutron Intensity: $I(Q) \propto (\Delta\rho^2 + \underline{p_0{}^2 \Delta M^2 \sin^2\alpha})\,|f(Q)|^2$

Magnetic scattering from $\mathbf{\Delta M} \perp \mathbf{Q}$ *only*!

SANS 2D Patterns with & without Magnetic Field

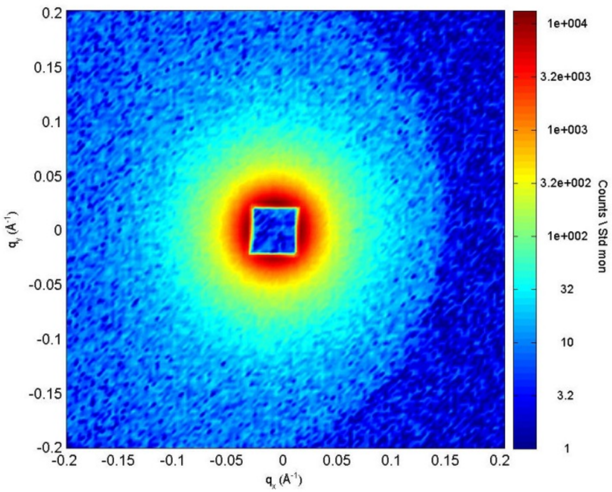

2m, B=0

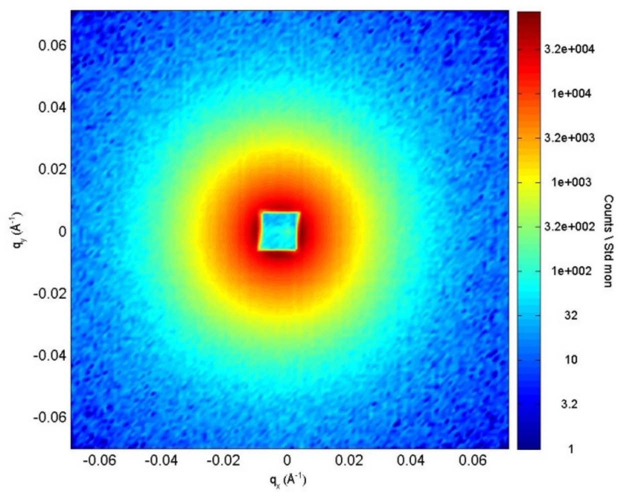

6m, B=0

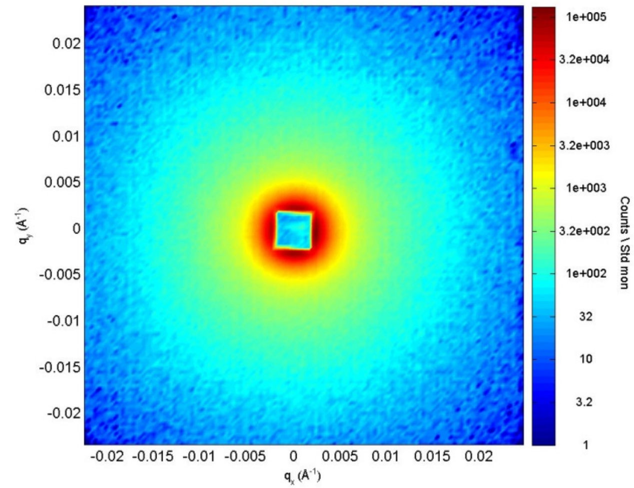

18m, B=0

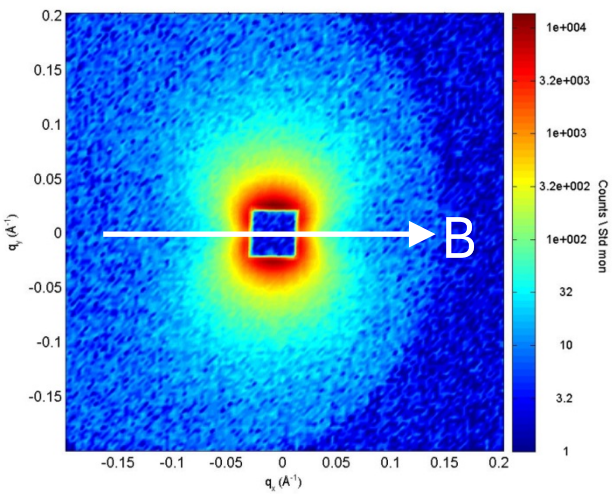

2m, B=1.1 T

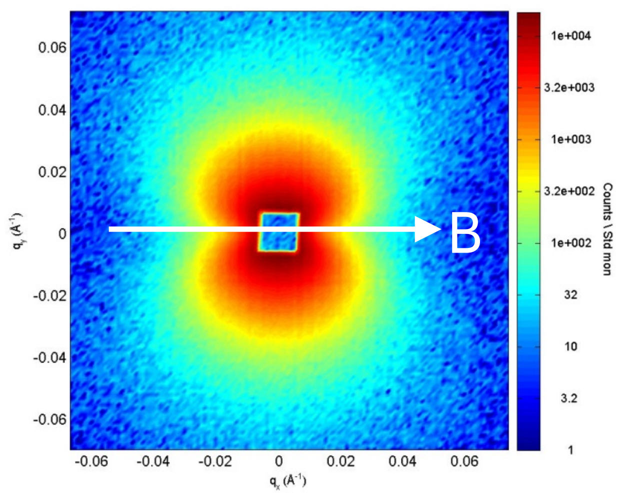

6m, B=1.1 T

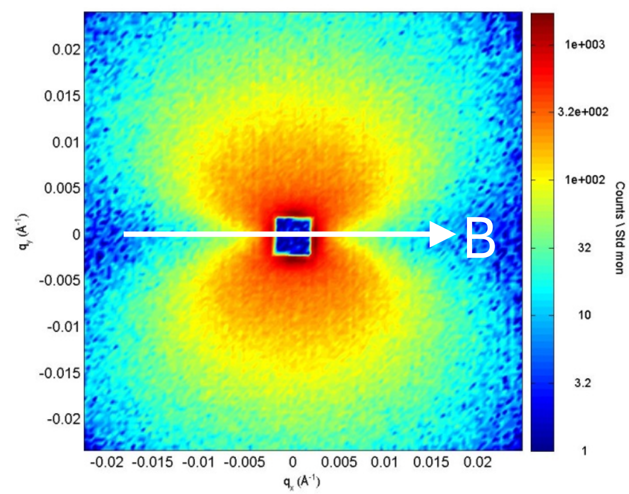

18m, B=1.1 T

Fe-Cu, AQ, 8% deformed, aged for 96h at 550°C

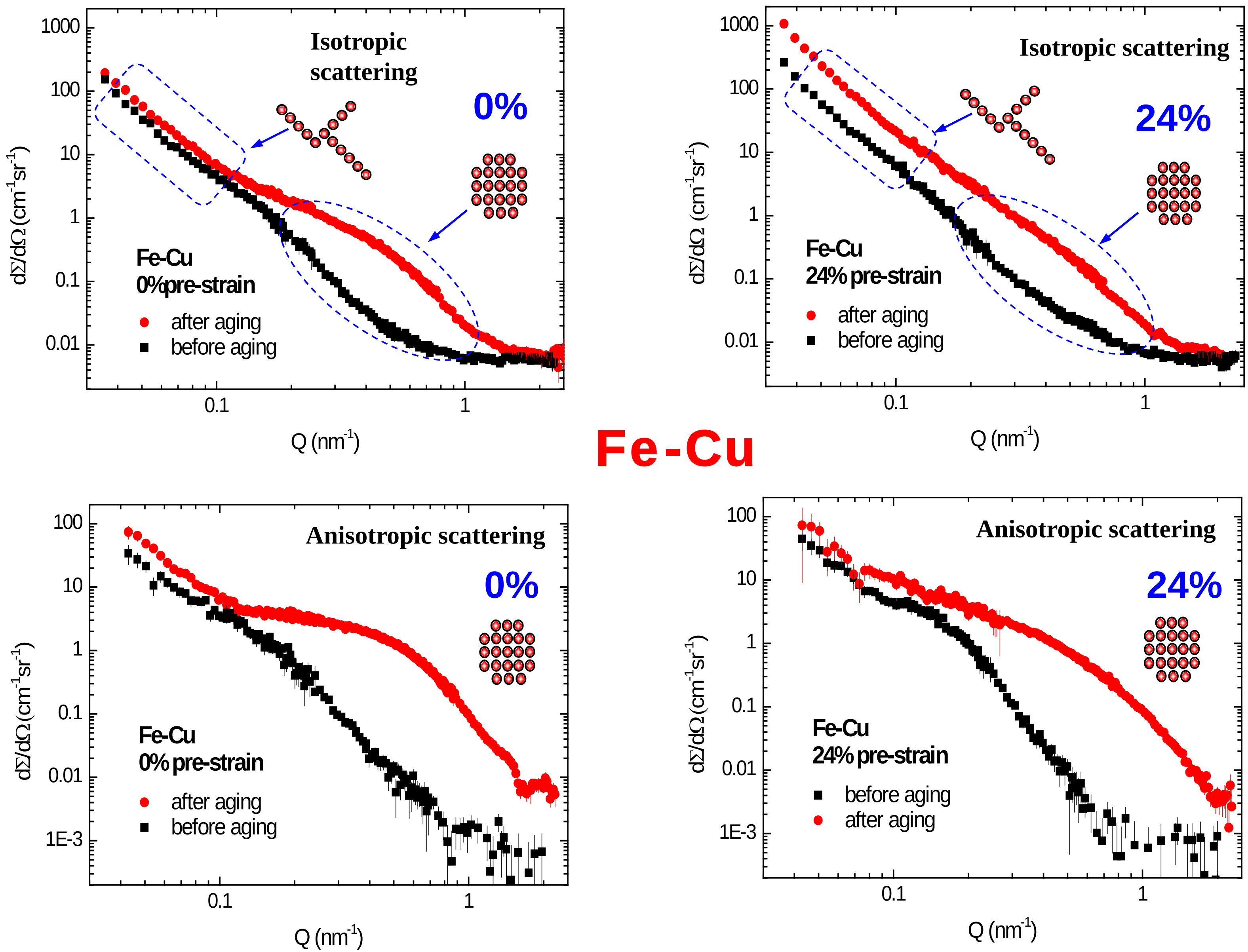

Isotropic (nuclear) & anisotropic (magnetic) SANS intensity before/after aging at 550 ^{o}C for 12 h with 0% and 24% deformation

TEM after 12 h of aging at 550 °C

0 % deformation

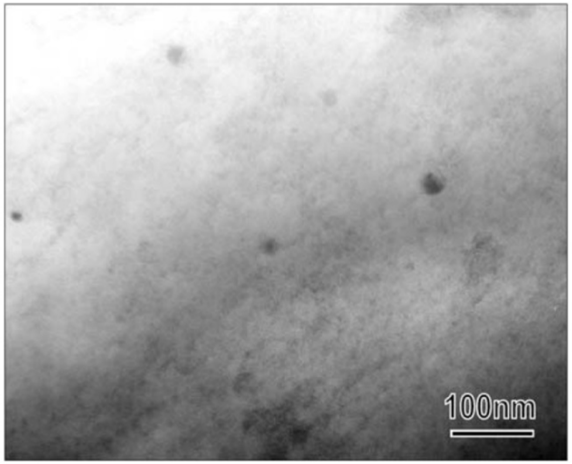

He *et al.*,
Phys. Rev. B 82 (2010) 174111.

8 % deformation

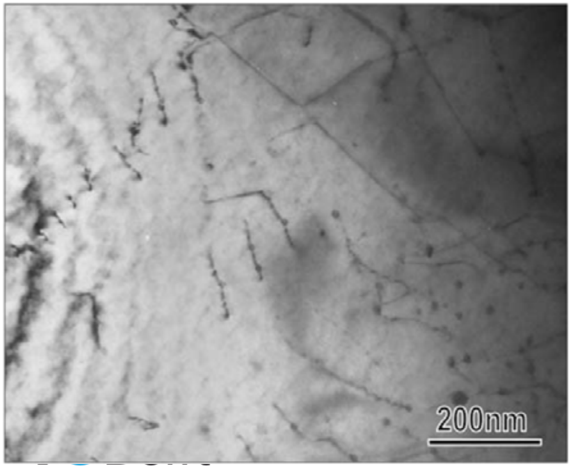

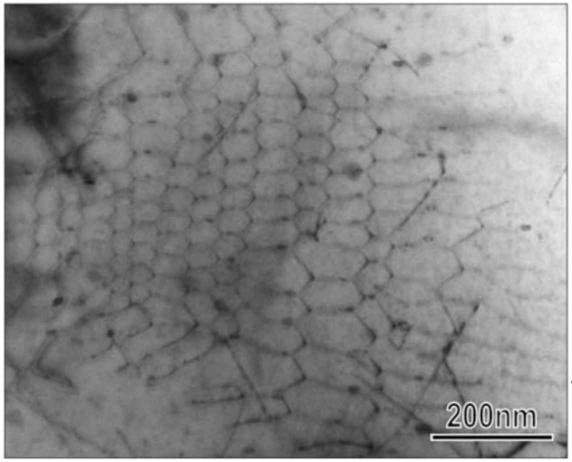

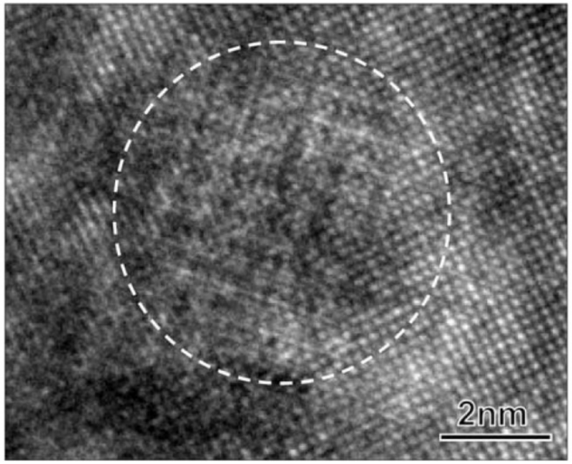

Phase fraction of Cu precipitates

Invariant: $$Q_{0,i} = \int_0^\infty \left(\frac{d\Sigma}{d\Omega}\right)_i Q^2 dQ = 2\pi^2 (\Delta\rho_i)^2 f_V (1 - f_V)$$

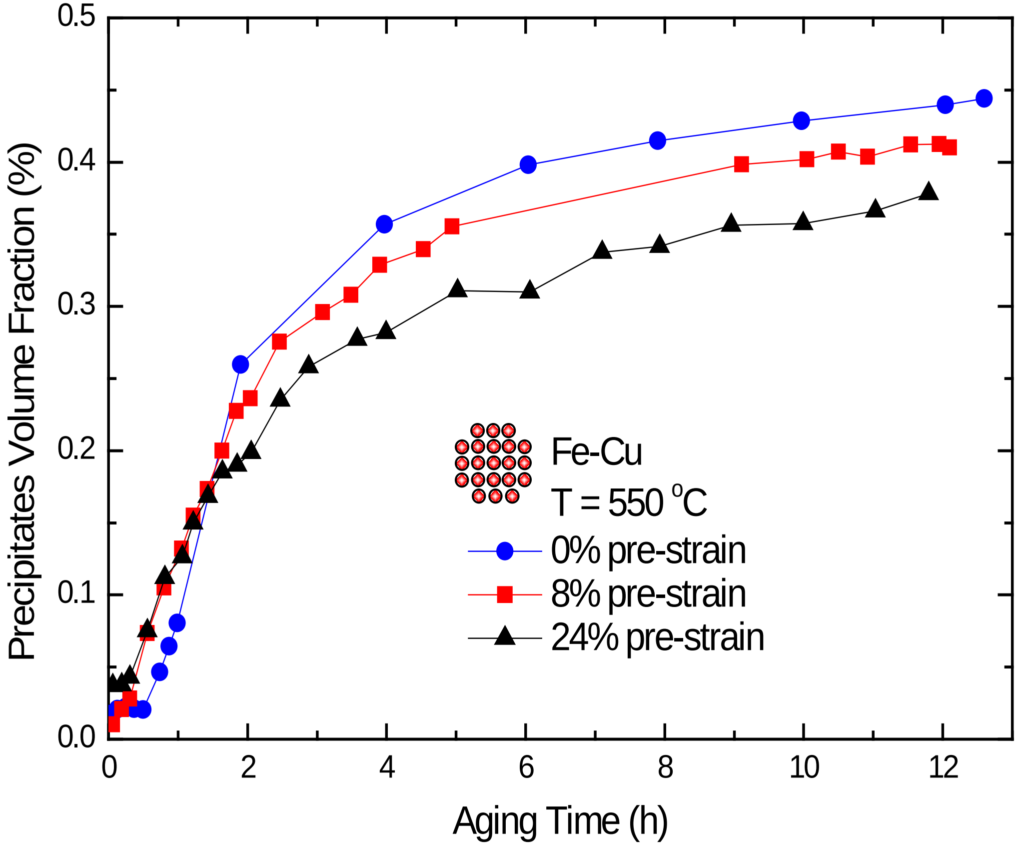

Profile fitting of the SANS curve

$$\left(\frac{d\Sigma}{d\Omega}\right)(Q)=(\Delta\rho)^2\int_0^\infty D_N(R)V^2(R)P(Q,R)\,dR$$

Theoretical estimate contrast:

Nuclear: $(\Delta\rho_{NUC})^2 = 2.2\times10^{28}$ m^{-4}

Magnetic: $(\Delta\rho_{MAG})^2 = 15.5\times10^{28}$ m^{-4}

$(\Delta\rho_{MAG})^2 \gg (\Delta\rho_{NUC})^2$

Particle volume: $V(R)=4\pi R^3/3$

Log-normal number distribution of particles:

$$D_N(R)=\frac{N_p}{R\sigma\sqrt{2\pi}}\exp\left(-\frac{\left[\ln(R)-\ln(R_m)\right]^2}{2\sigma^2}\right)$$

Square of formfactor:

$$P(Q,R)=\left|F(Q,R)\right|^2=\left(3\frac{\sin(QR)-(QR)\cos(QR)}{(QR)^3}\right)^2$$

Time-resolved SANS measurements Fe-Cu

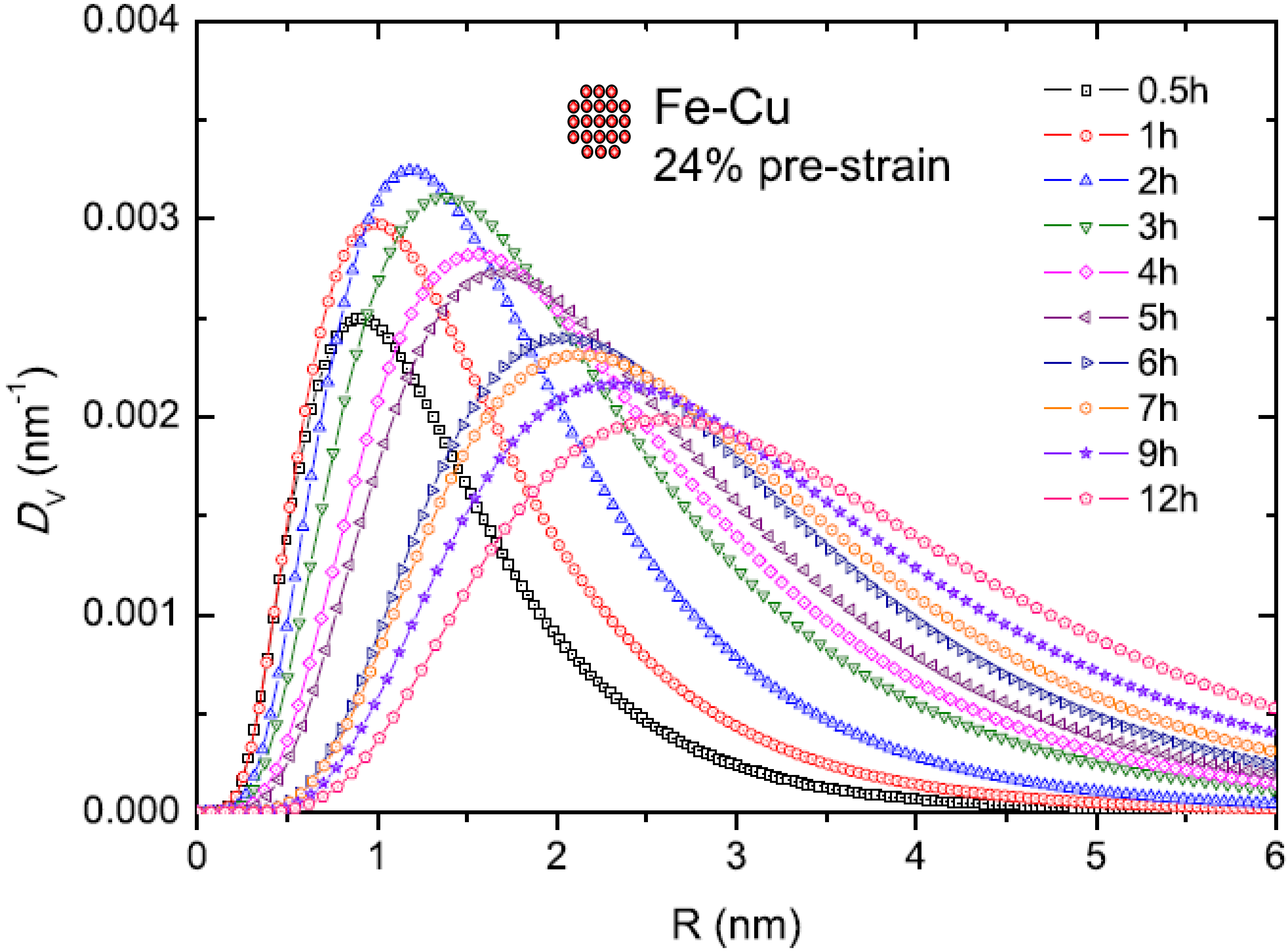

Time-resolved SANS measurements Fe-Cu

Structure evolution Cu precipitates during growth:

bcc → **9*R*** → **3*R*** → ***fcc***

bcc : $R < 5$ nm

9*R* : 5 nm $< R <$ 16 nm

3R & fcc : $R > 16$ nm

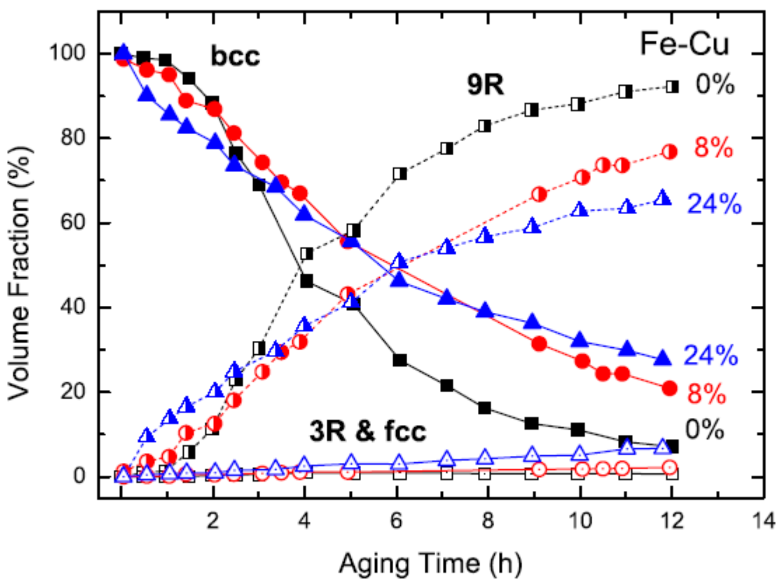

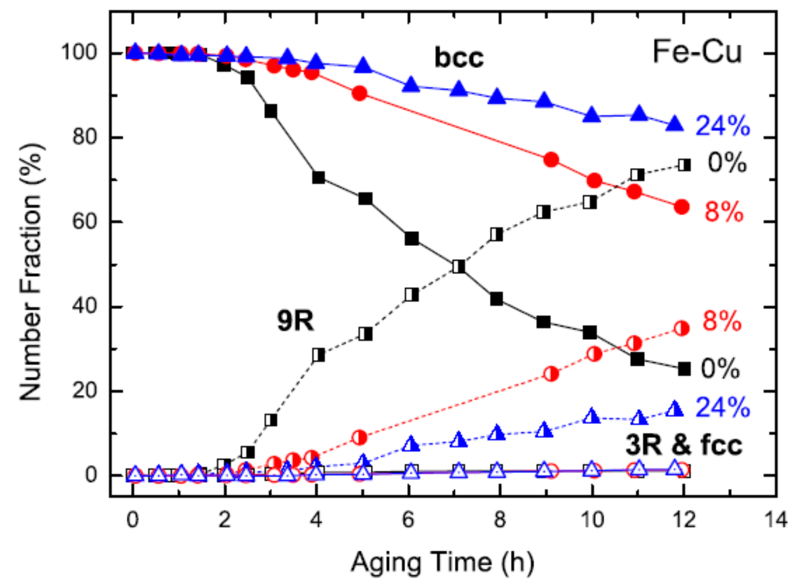

Time-resolved SANS measurements Fe-Cu

Network of Cu along dislocations/interfaces

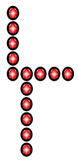

Porod constant K_p: $\lim_{Q\to\infty}[I(Q)] = K_p Q^{-4} + B$

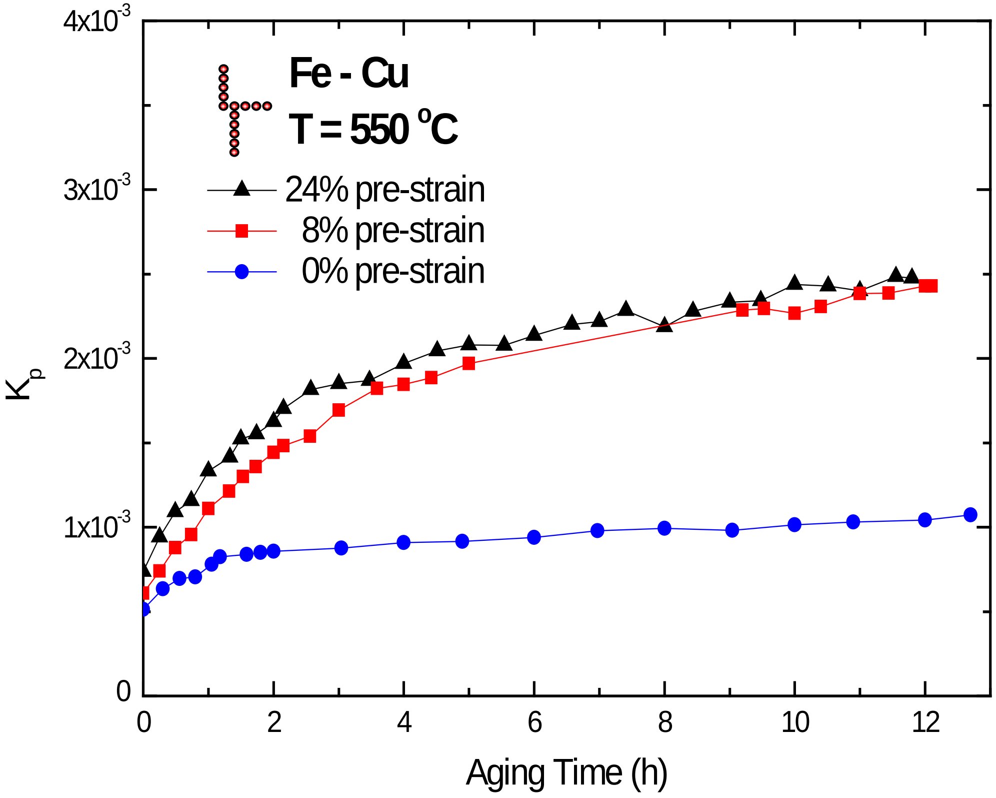

$$\boxed{K_p = 2\pi(\Delta\rho)^2 S_V}$$

with specific surface:

$$S_v = \frac{\text{interface area}}{\text{volume}}$$

Pre-strain leads to a strong Cu precipitation at dislocations/interfaces

Time-resolved ASAXS measurements undeformed Fe-Cu (8x enhanced contrast)

E = 7.106 keV
L = 20-30 μm

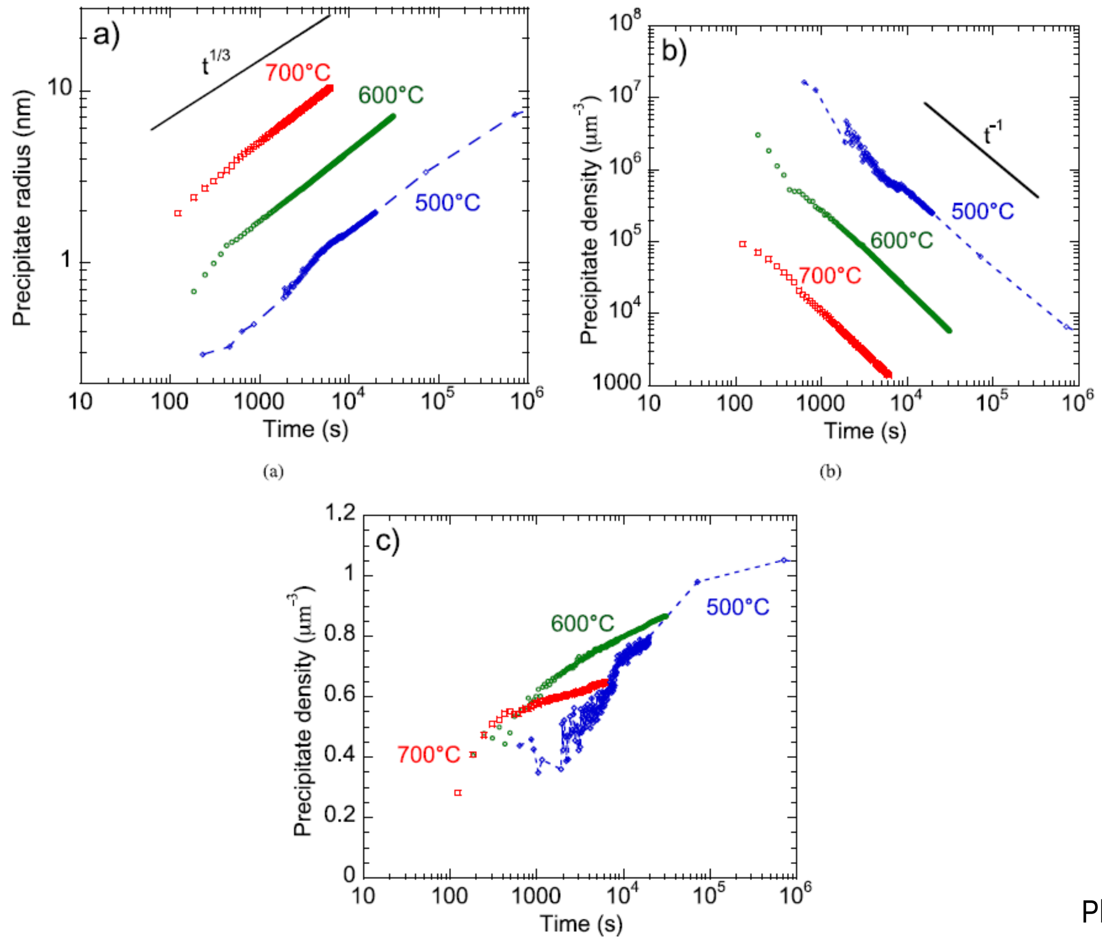

Perez *et al.*,
Philos. Mag. 85 (2005) 2197.

Example:

SANS on Au precipitation
in deformed Fe-Au alloys

Au precipitation in deformed Fe-Au (1 at.%)

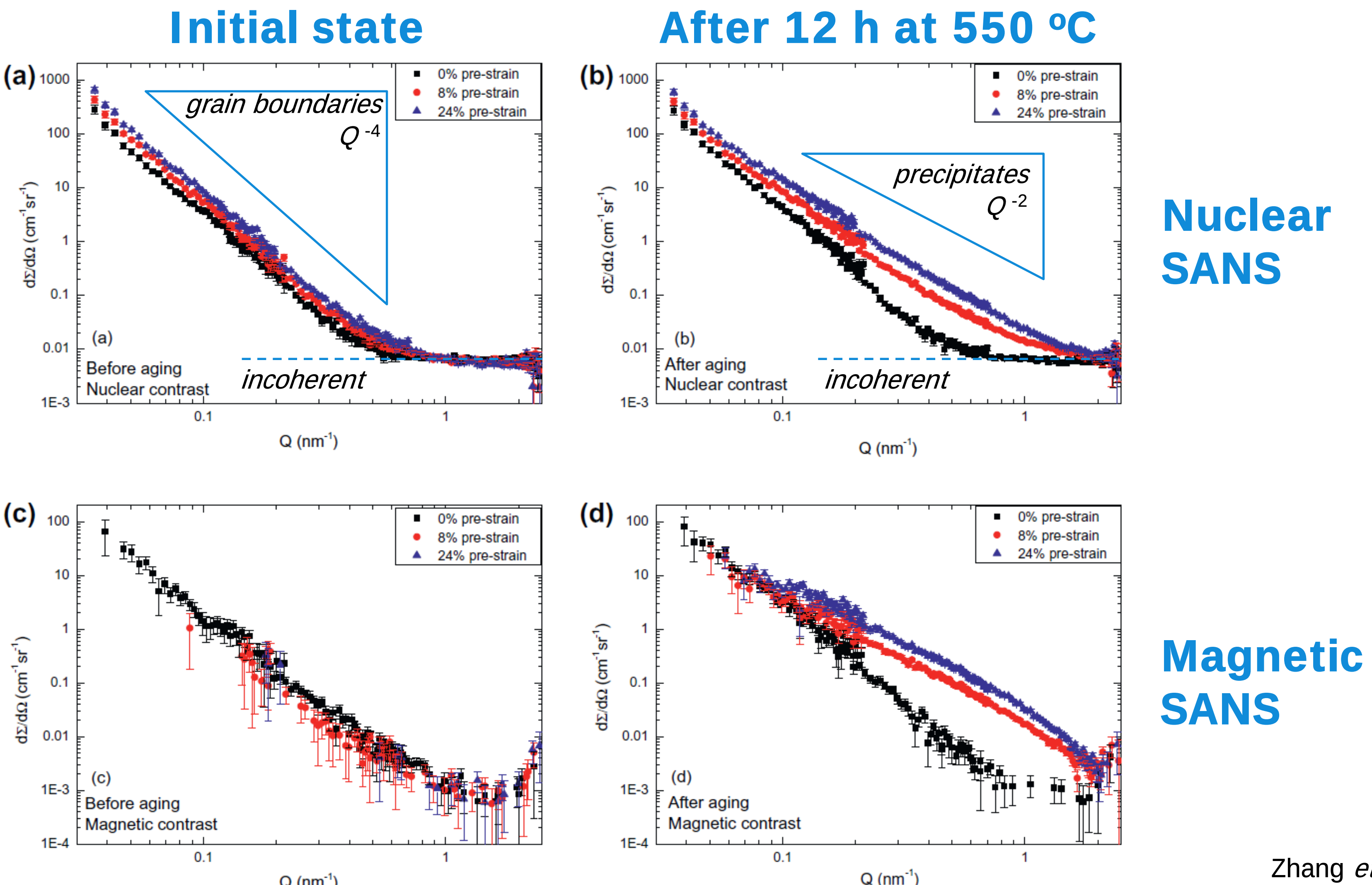

Zhang *et al.*,
Acta Mater. 61 (2013) 7009.

TEM of Au precipitates in Fe-Au after aging

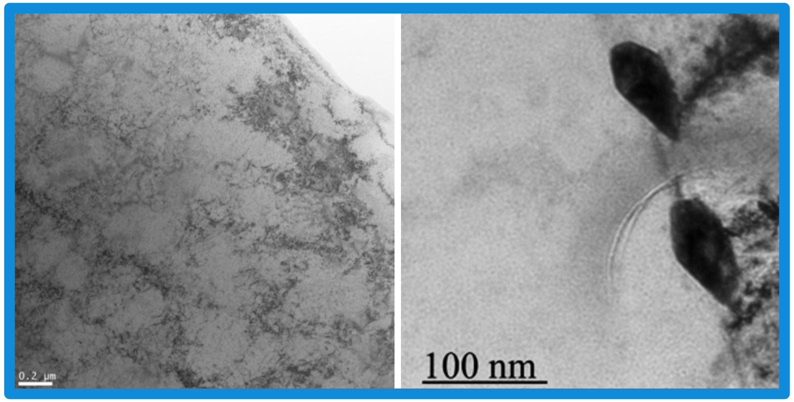

Fe-Au 0%, Pre-strain

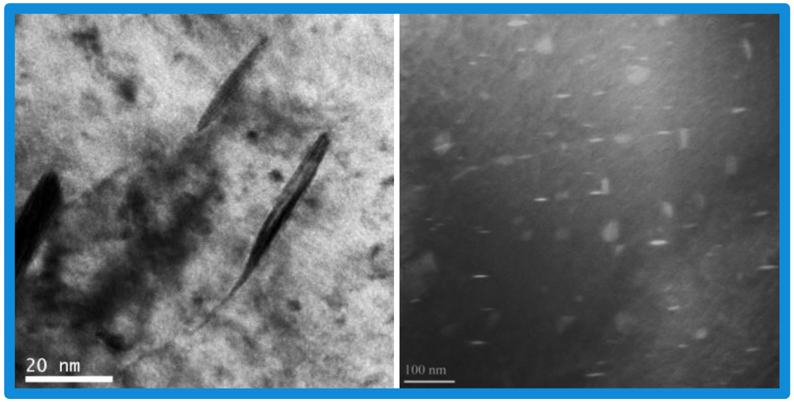

Fe-Au 24%, Pre-strain

- Undeformed: only along grain boundaries
- Deformed:
  1. along grain boundaries
  2. disk-like, closely connected to the dislocations

Zhang *et al.*,
Acta Mater. 61 (2013) 7009.

Disk-shaped precipitates

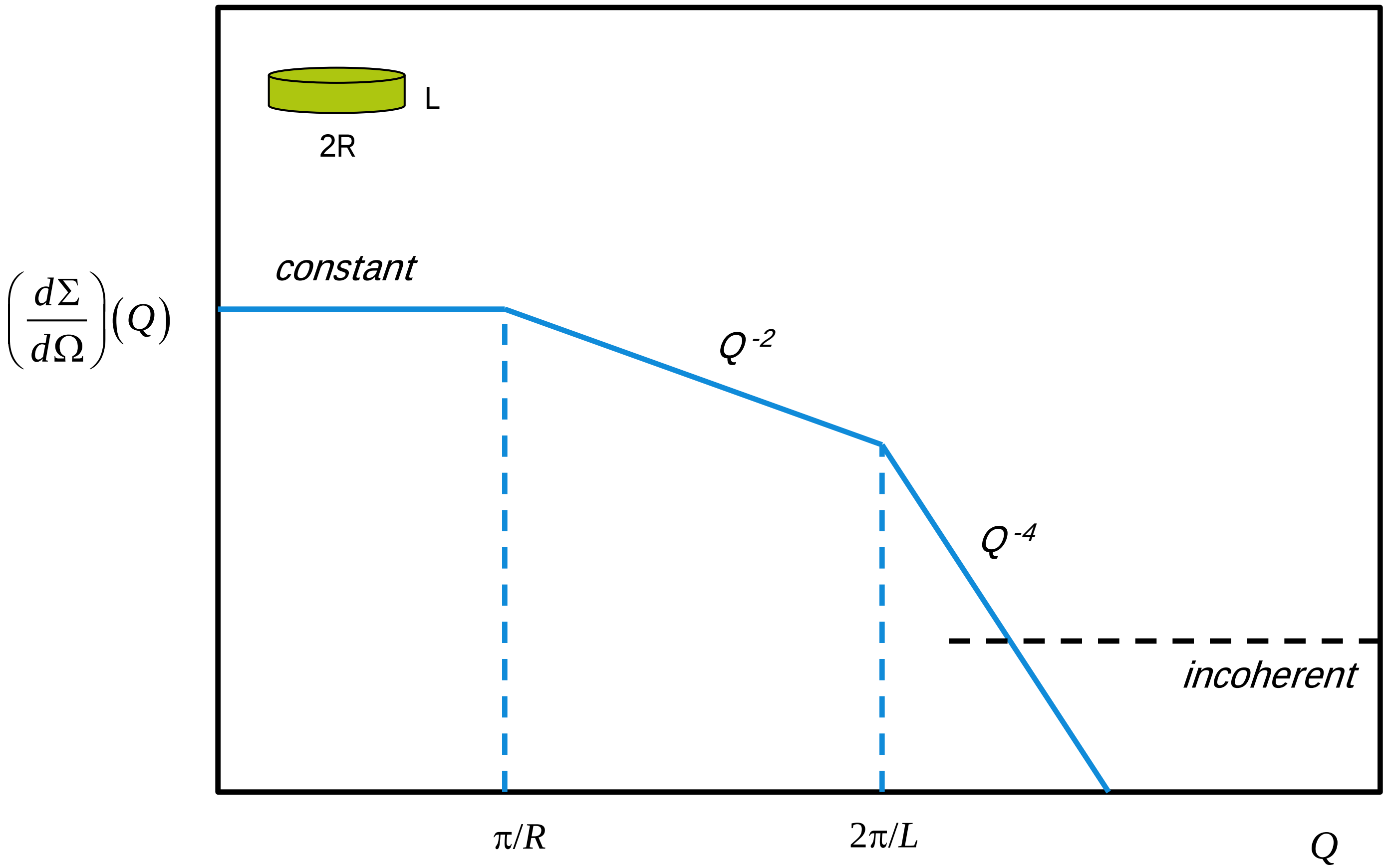

Phase fraction of Au precipitates

Invariant: $$Q_{0,i} = \int_0^\infty \left(\frac{d\Sigma}{d\Omega}\right)_i Q^2 dQ = 2\pi^2 (\Delta\rho_i)^2 f_V (1 - f_V)$$

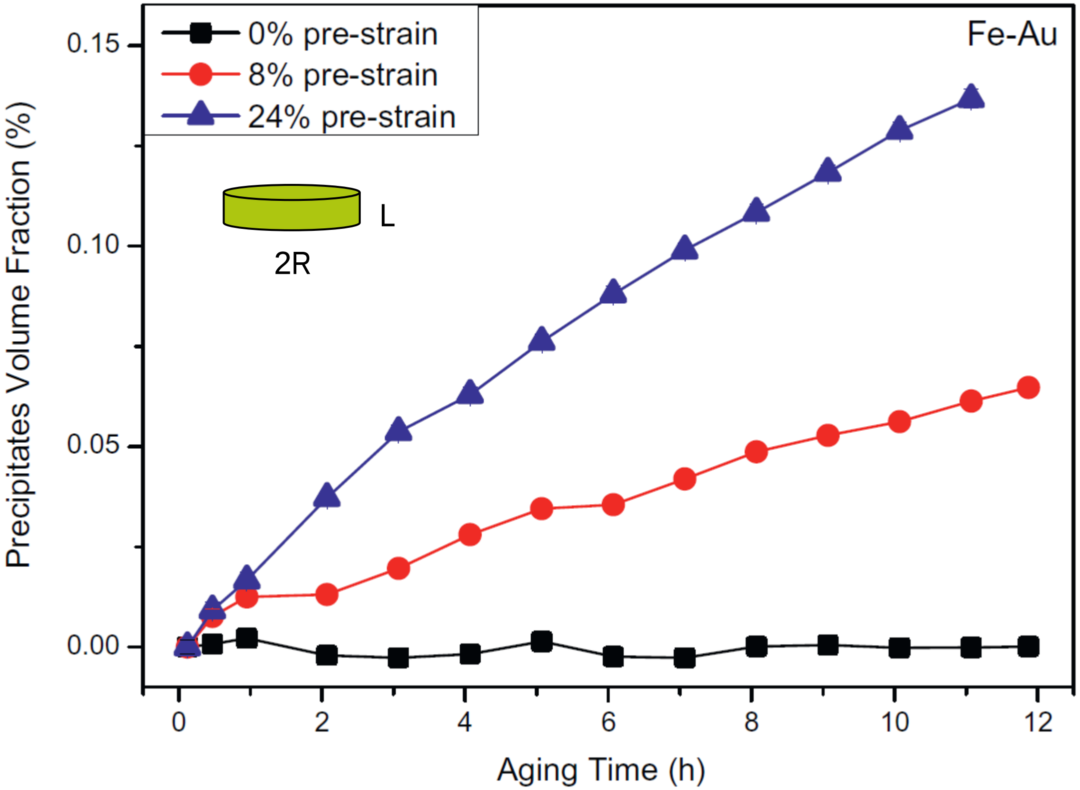

Specific surface (S/V) circular caps Au precipitates

For disk-shaped precipitates with $\pi / R \ll Q \ll 2\pi / L$:

$$\left(\frac{d\Sigma}{d\Omega}\right)(Q) = C_2 Q^{-2} + C_0 \quad \text{where} \quad \boxed{C_2 = 4\pi\left(\Delta\rho\right)^2 f_V{}^2 / S_{vc}}$$

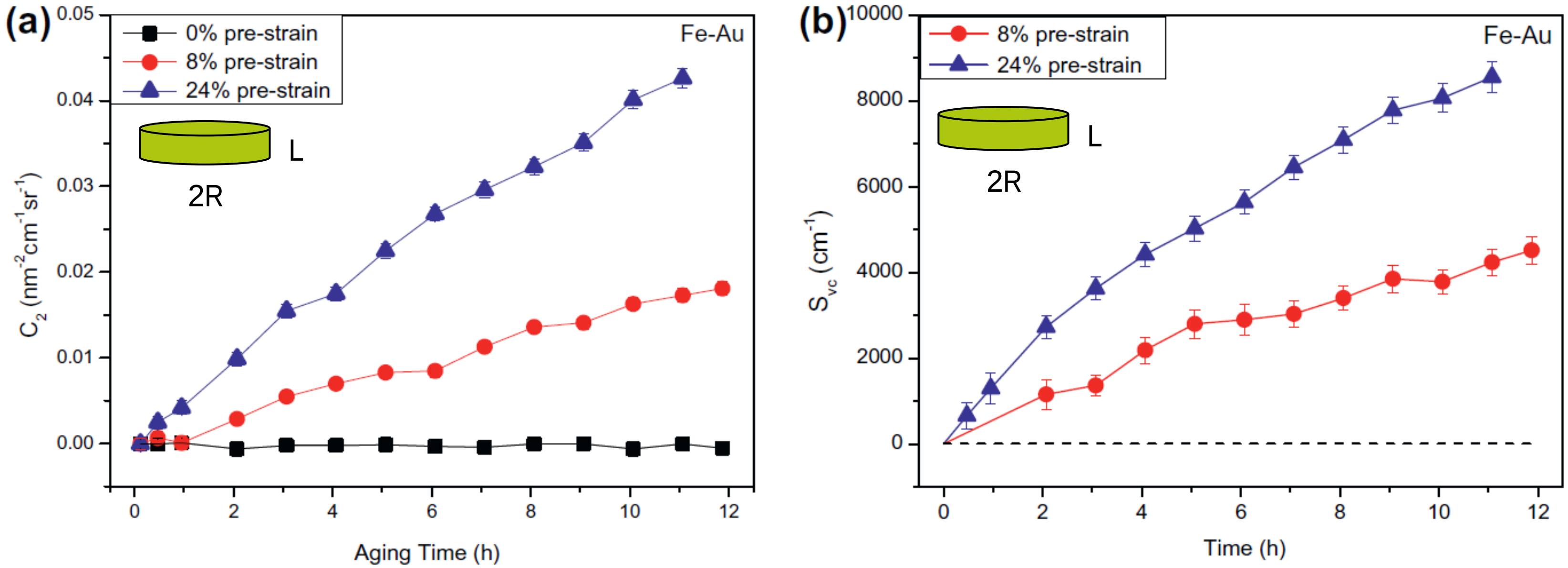

Specific surface for monodisperse disks:

$$S_{vc} = 2\pi R^2 N_p = 2 f_V / L \rightarrow C_2 = 2\pi\left(\Delta\rho\right)^2 f_V L$$

Profile fitting of the SANS curve

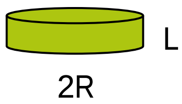

$$\boxed{\left(\frac{d\Sigma}{d\Omega}\right)(Q) = (\Delta\rho)^2 \int_0^\infty D_N(R) V^2(R) P(Q,R)\, dR}$$

Particle volume: $V(R) = \pi R^2 L = 2\pi R^3 / \varepsilon$ with aspect ratio $\varepsilon = 2R/L$

Log-normal number distribution of particles:

$$D_N(R) = \frac{N_p}{R\sigma\sqrt{2\pi}} \exp\left(-\frac{\left[\ln(R) - \ln(R_m)\right]^2}{2\sigma^2}\right)$$

Orientation-averaged square of formfactor:

$$P(Q,R) = \int_0^{\pi/2} |F|^2 \sin(\alpha)\, d\alpha = \int_0^{\pi/2} \left(\frac{2J_1(QR\sin(\alpha))}{QR\sin(\alpha)} \frac{\sin(QL\sin(\alpha)/2)}{QL\sin(\alpha)/2}\right)^2 \sin(\alpha)\, d\alpha$$

Profile fitting of the SANS curve

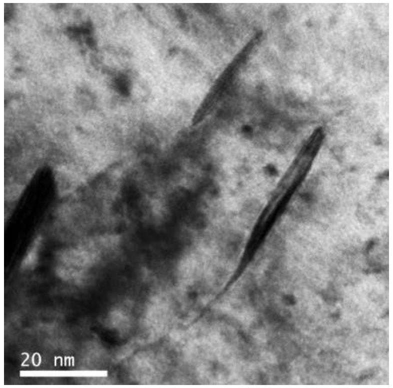

$$\varepsilon = 2R / L \approx 8$$

SANS

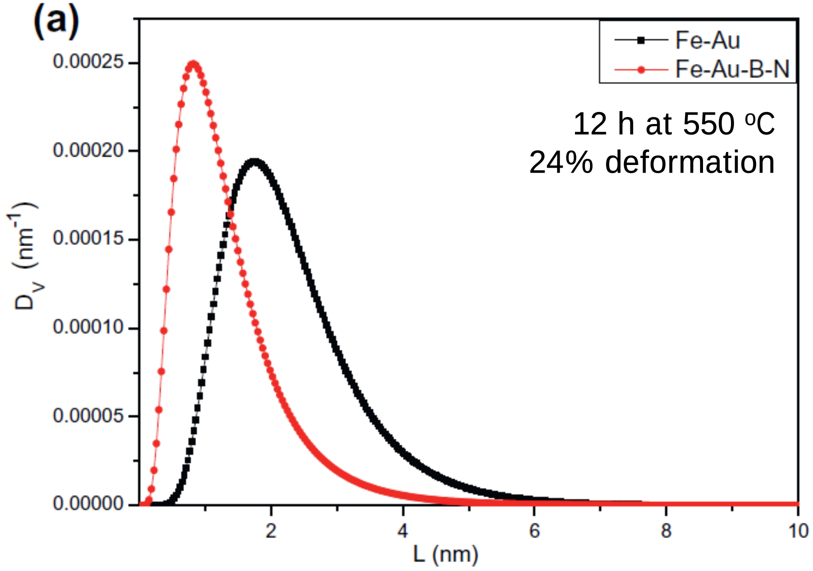

TEM

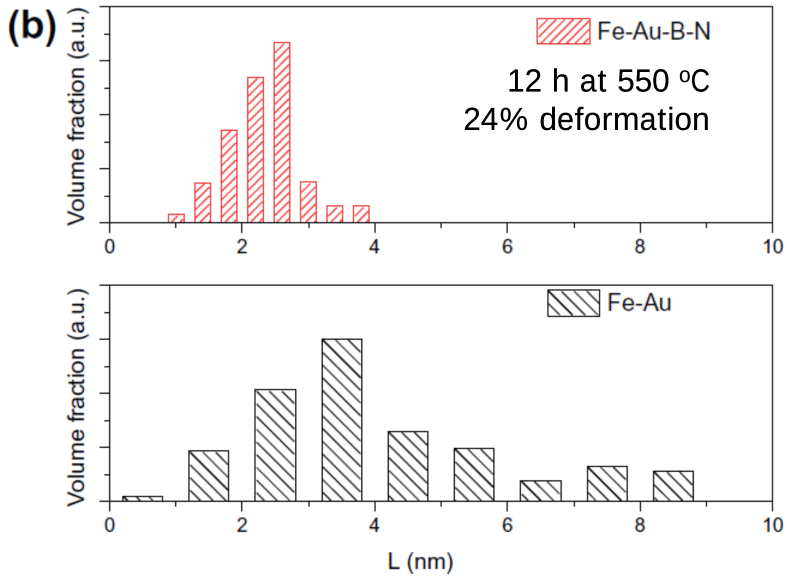

Au segregation at (sub)grain boundaries

For Porod scattering: $Q \gg \pi / R$ and $Q \gg 2\pi / L$:

$$\left(\frac{d\Sigma}{d\Omega}\right)(Q) = C_2 Q^{-4} + C_0 \quad \text{where} \quad \boxed{C_4 = 2\pi\left(\Delta\rho\right)^2 S_v}$$

Specific surface S_v = interfacial area per unit volume

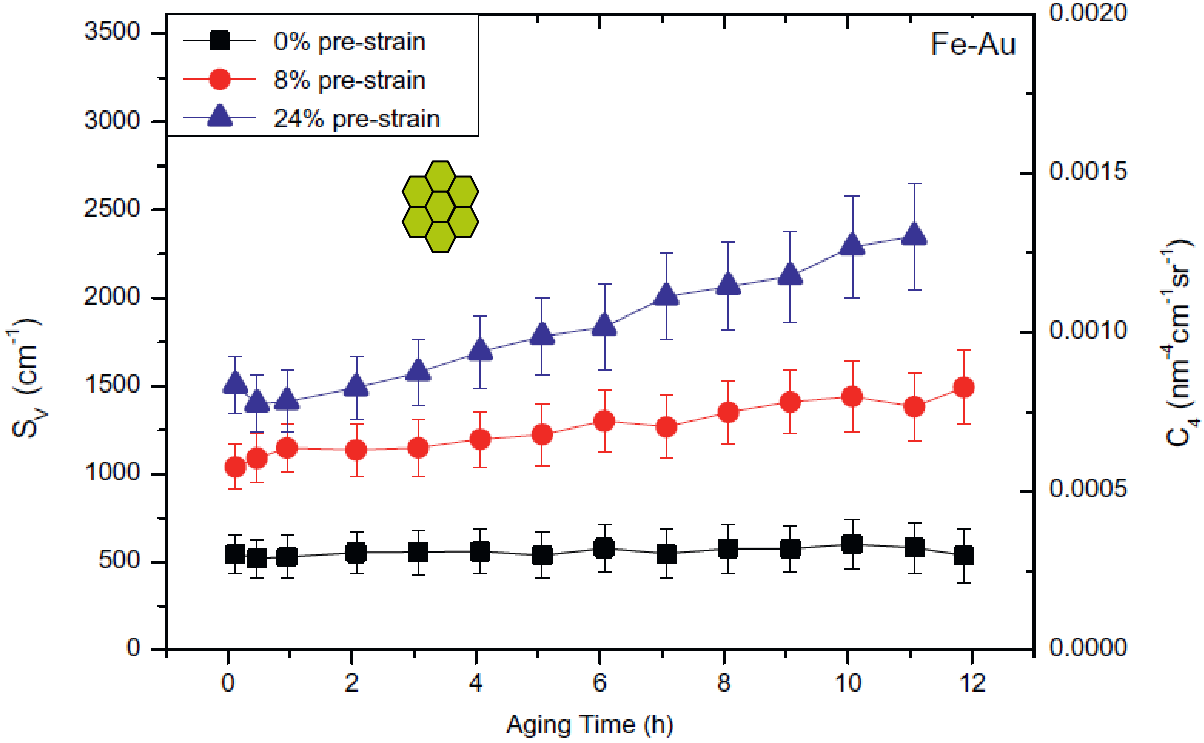

Example:

SAXS on $(Fe,Cr)_7C_3$ carbides and dislocation structures in low-Cr steel

SAXS pattern:

E = 17 keV
λ = 0.729 Å

Heat treatment:

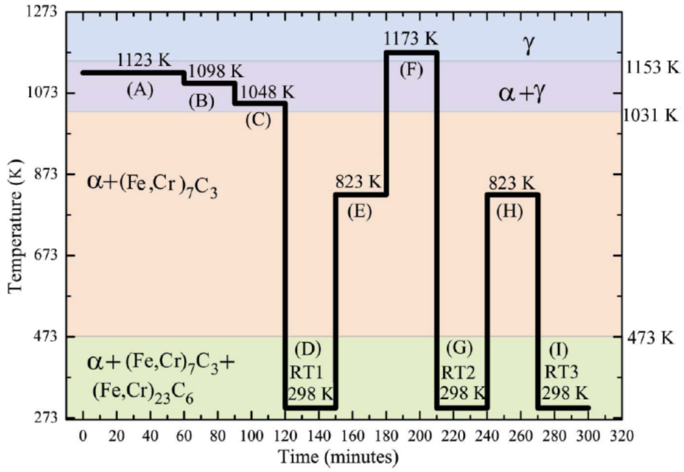

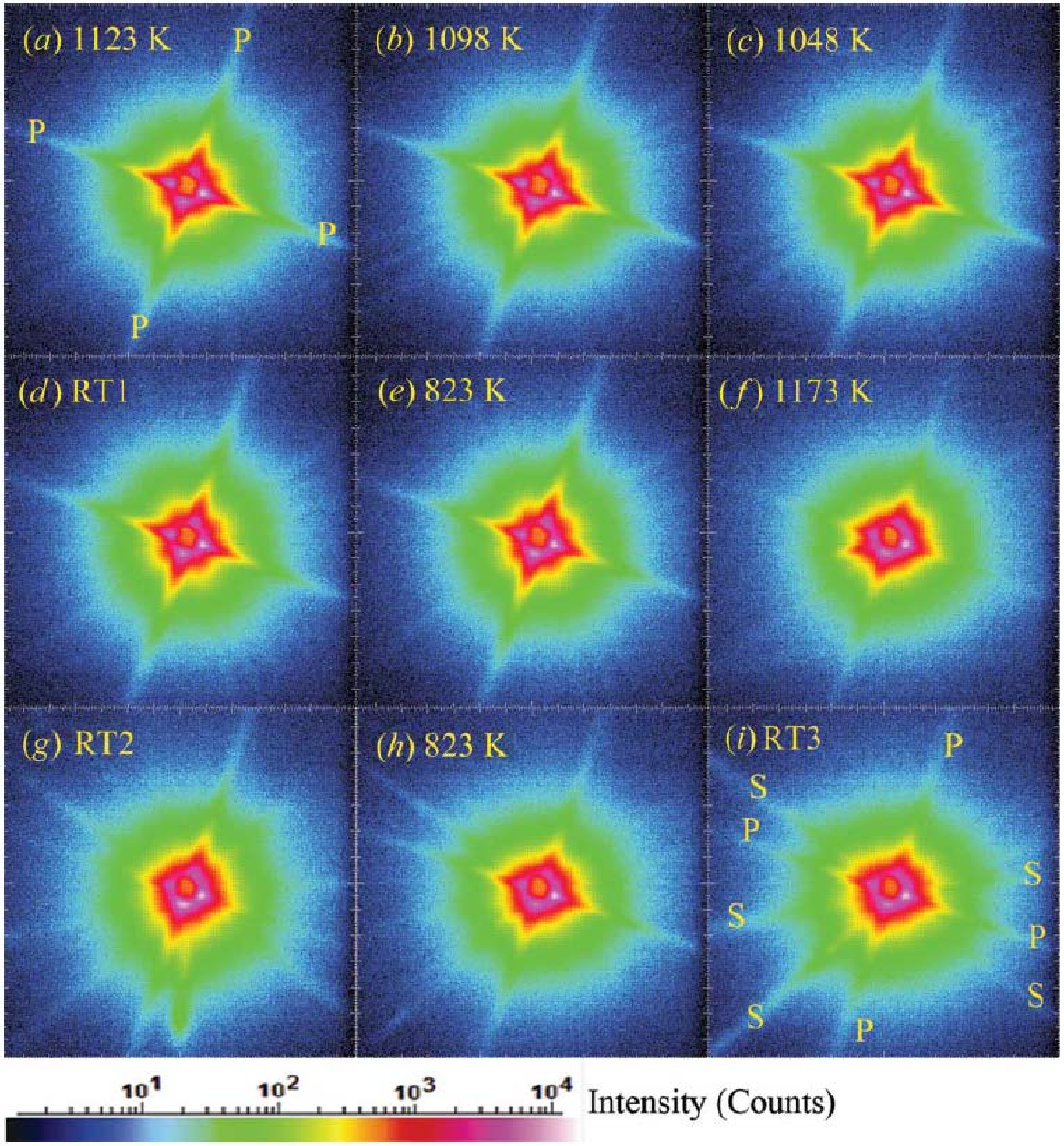

Isotropic → ***precipitate***
Streaks → ***dislocations***

Gözde Dere *et al.*,
J. Appl. Cryst. 46 (2013) 181.

Isotropic SAXS profile

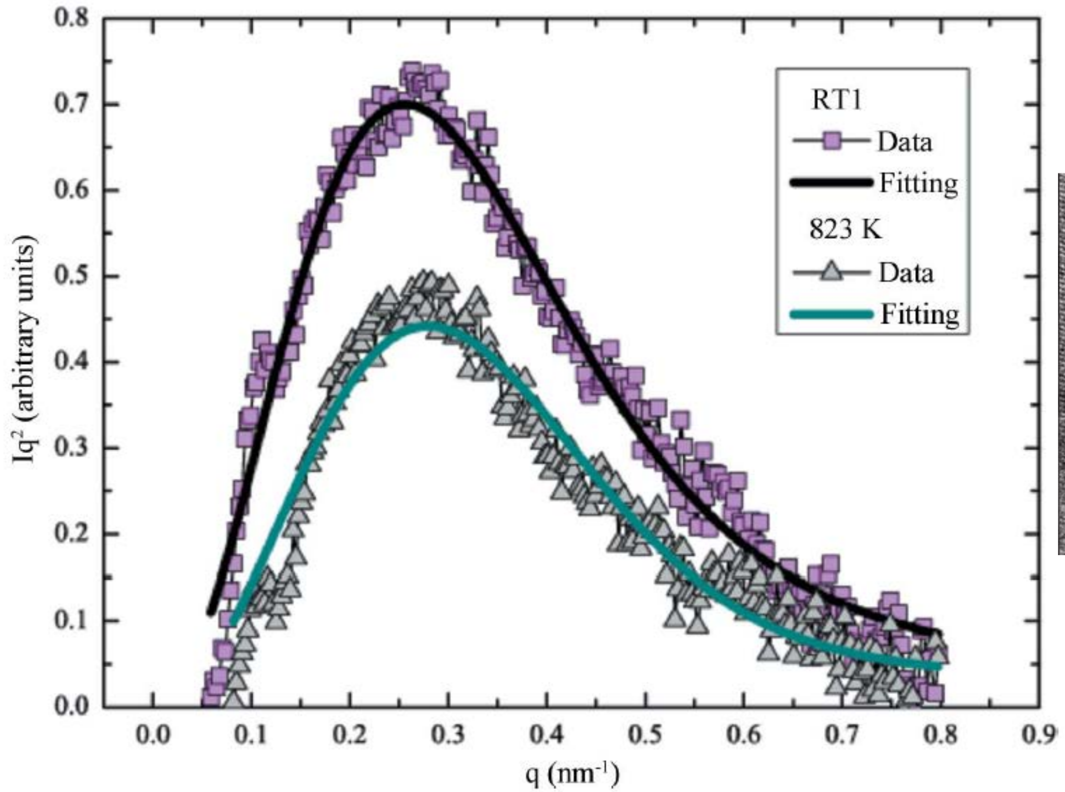

TEM

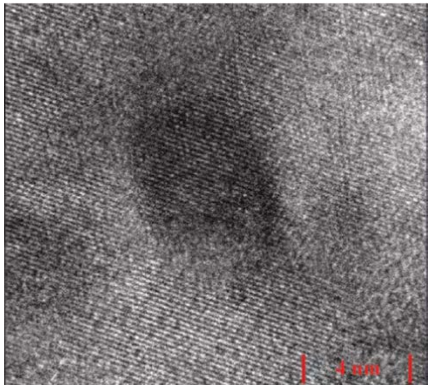

	R_m (nm)	s	f_v (%)	N (m^{-3})
RT	4.74	0.33	0.013	2.98×10^{22}
823 K	5.25	0.26	0.010	1.64×10^{22}

Gözde Dere *et al.*,
J. Appl. Cryst. 46 (2013) 181.

Lognormal size distribution: $f(R) = \frac{1}{sR(2\pi)^{1/2}} \exp\left\{-\frac{1}{2}\left[\frac{\ln(R/R_m)}{s}\right]^2\right\}$

Streaks in SAXS profiles

Small-angle scattering from dislocations

Edge dislocation

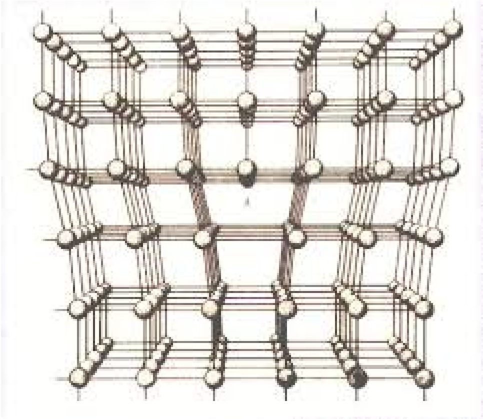

Strain field
(= Density variation)

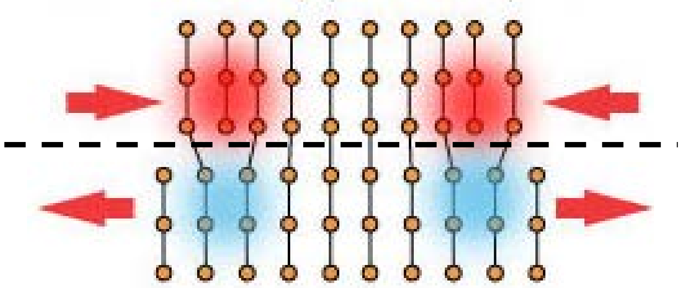

For dislocation walls (Long & Levine, Acta Cryst. A 61 (2005) 557):

$$I = A^2\left[cL + F_t\left(Q_t, L\right)F_w\left(Q_w, L\right)\right]$$

⇨ Strongly anisotropic scattering along (Q_w) and perpendicular (Q_t) to the wall.

Streaks in SAXS profiles
Correlation to simultaneous X-ray Diffraction

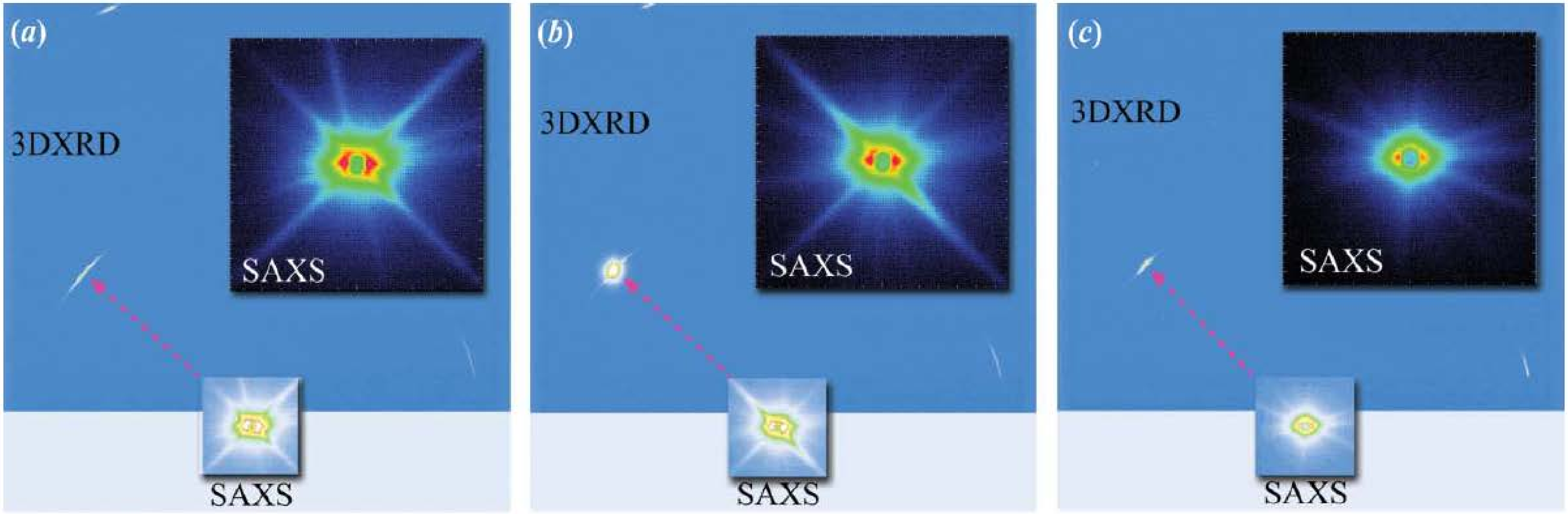

Gözde Dere *et al.*,
J. Appl. Cryst. 46 (2013) 181.

The data provide direct information that links:
the matrix phase structure, dislocations and nucleated precipitate.

Streaks in SAXS profiles
Correlation to simultaneous X-ray Diffraction

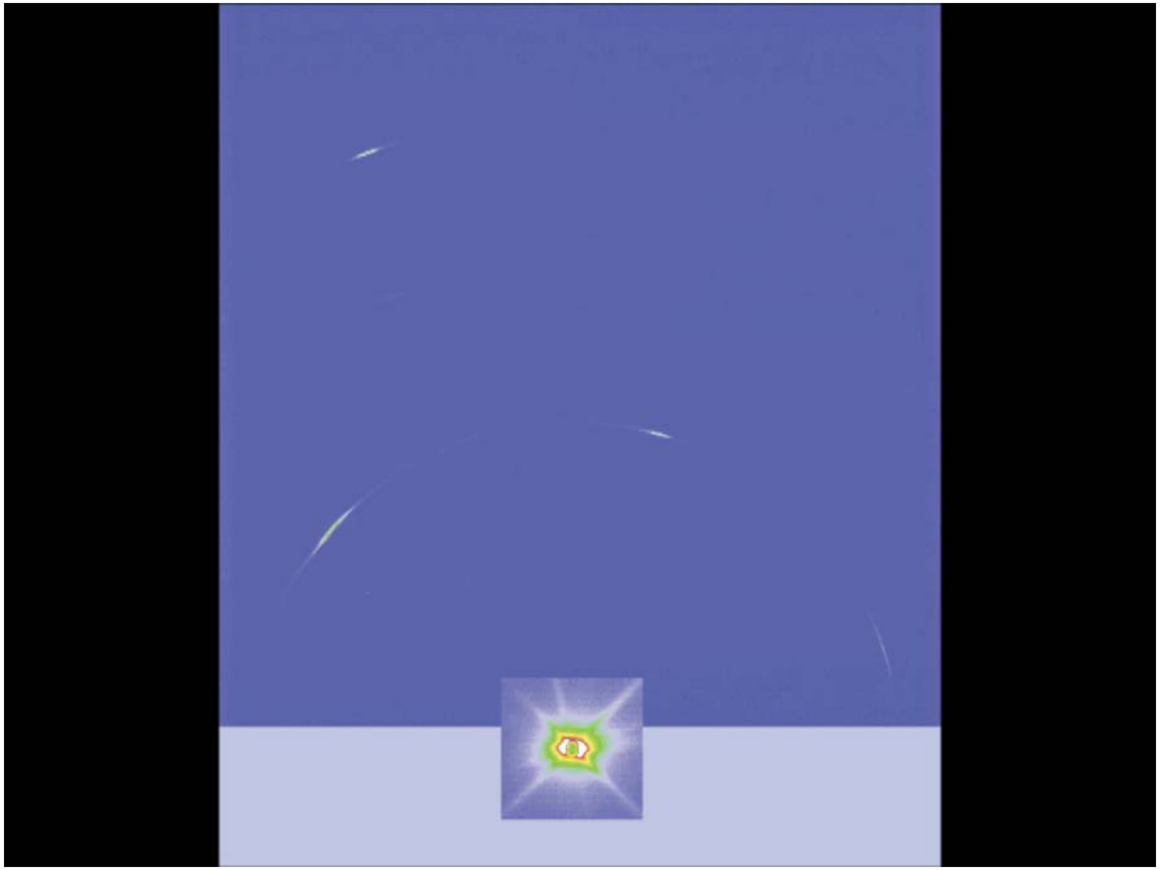

Gözde Dere *et al.*,
J. Appl. Cryst. 46 (2013) 181.

Example:

SANS on the magnetic flux-line lattice of superconducting UPt_3

Small Angle Neutron Scattering

Magnetic
flux-line lattice
in superconductor

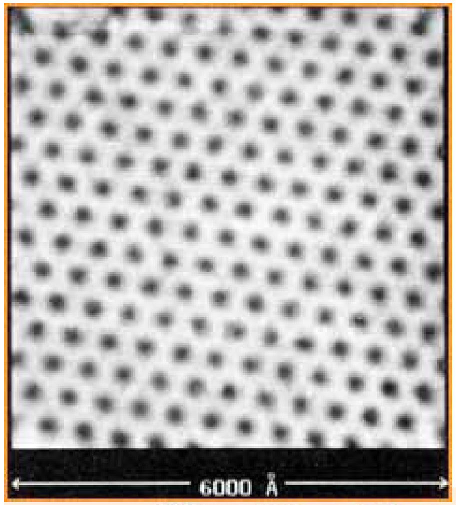

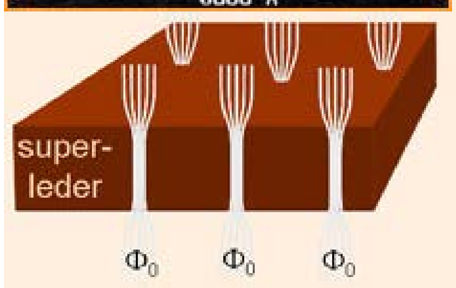

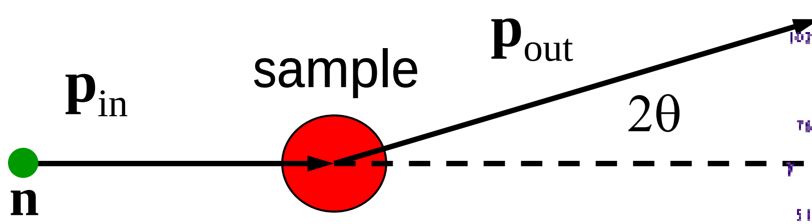

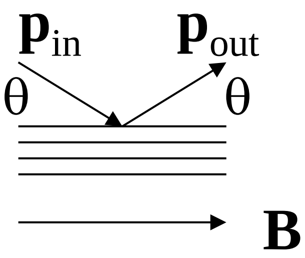

Diffraction pattern
(superconducting Nb)

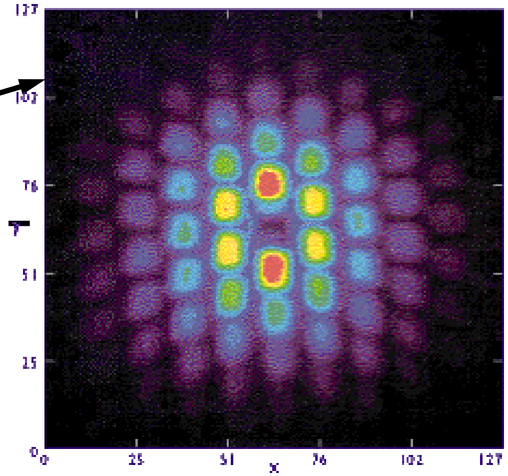

$$I(\mathbf{Q}) \propto |\, f(\mathbf{Q}) \,|^2$$

$f(\mathbf{Q})$ = form factor
field profile

Magnetic Flux-Line Lattice

Flux quantum: $\Phi_0 = h/2e = 2.07\times10^{-15}\ \mathrm{Tm}^2$

$$S = \Phi_0/B = (\sqrt{3}/2)\, a^2 = (2/\sqrt{3})\, d_{10}{}^2$$

$$\boxed{d_{10} = \sqrt{(\sqrt{3}/2)(\Phi_0/B)} = 423.4\ \text{Å}/\sqrt{B\,[\mathrm{T}]}}$$

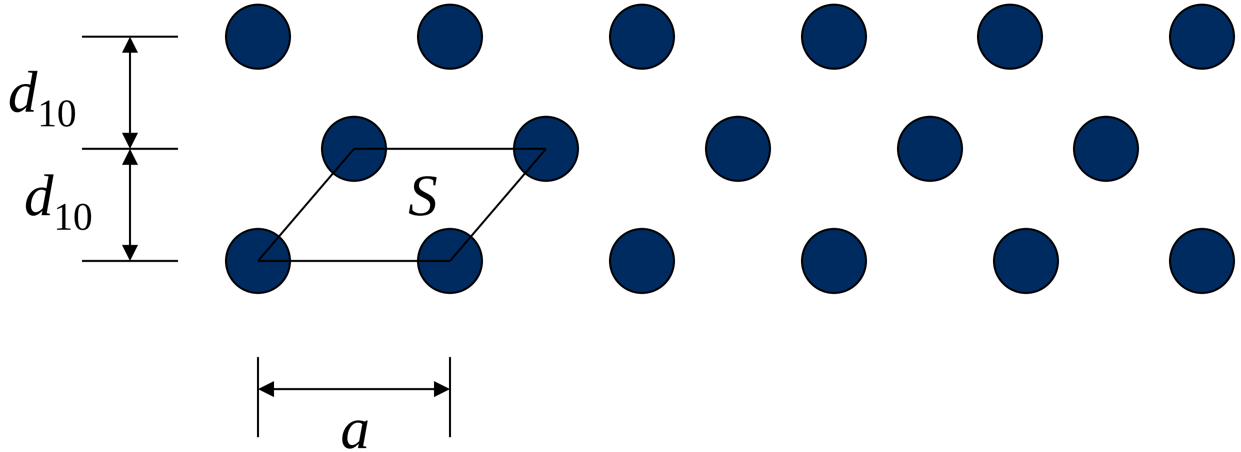

Unconventional superconductivity in UPt_3

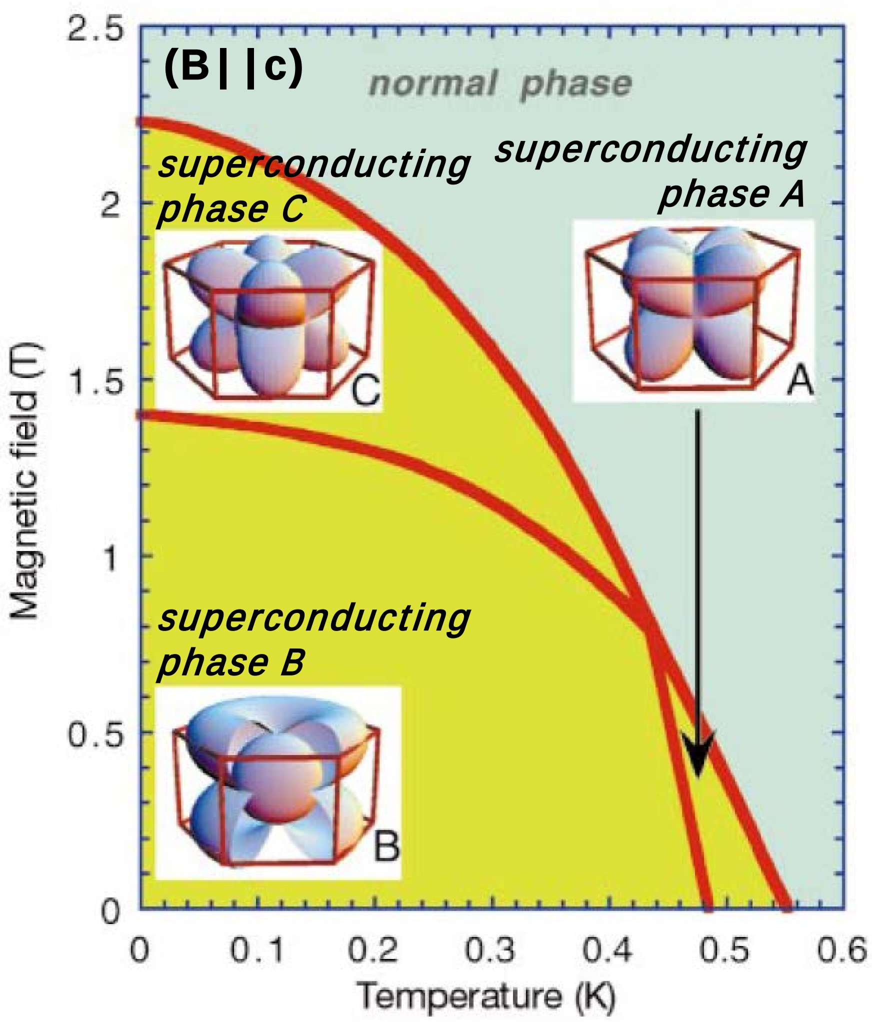

Huxley *et al.*, Nature 406 (2000) 160.

Flux-Line Lattice UPt_3 (B||c)

Normal State

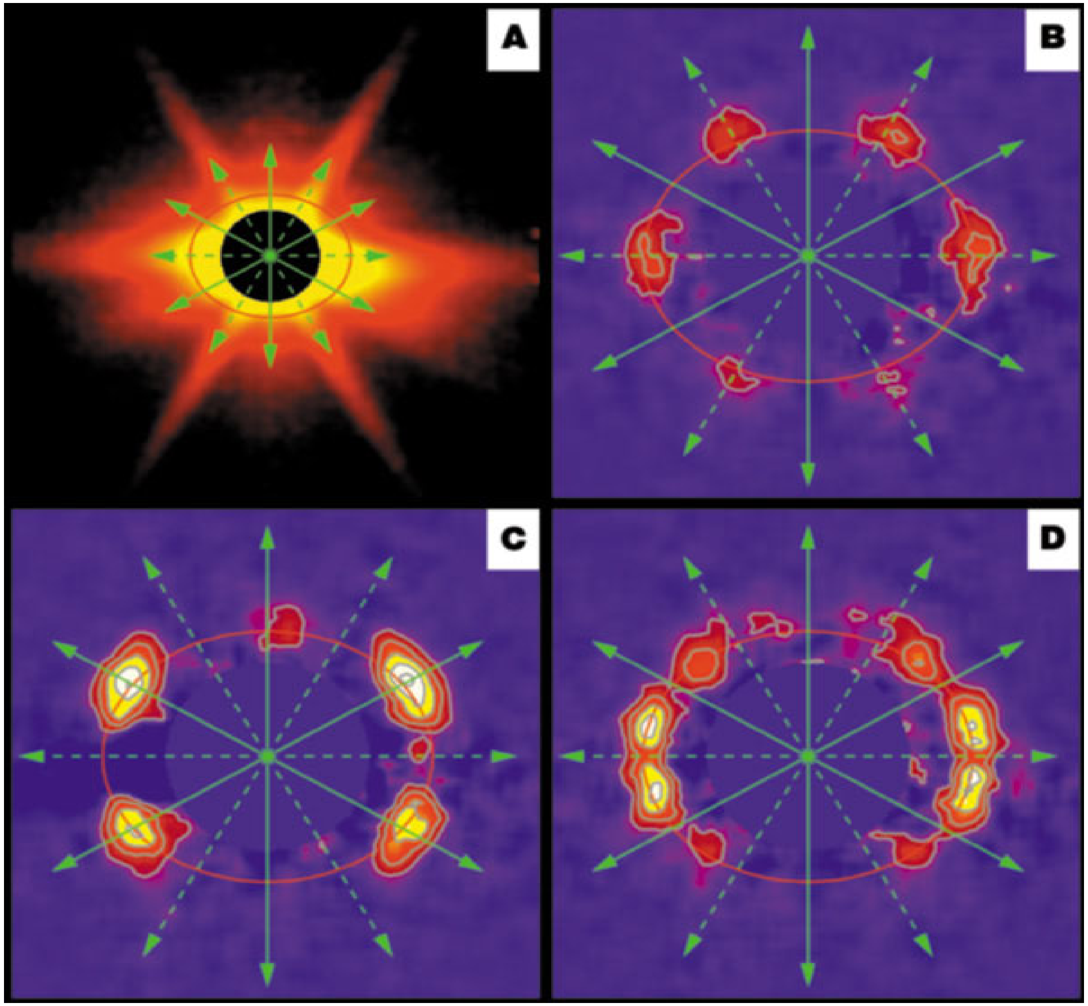

Field Cooled

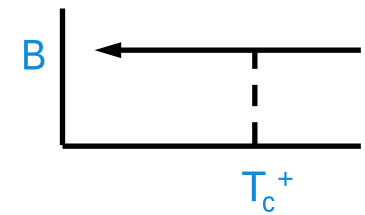

Zero-Field Cooled

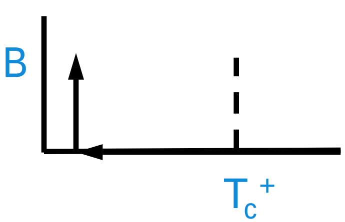

T_Q = 475 mK

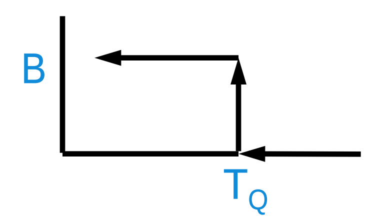

Huxley *et al.*, Nature 406 (2000) 160.

Further reading SAXS/SANS on metals:

P. Fratzl, *Small-angle scattering in materials science – a short review of applications in alloys, ceramics and composite materials,* J. Appl. Cryst. 36 (2003) 397-404.

G. Kostorz, *Small-Angle Scattering Studies of Phase Separation and Defects in Inorganic Materials, J. Appl. Cryst.* 24 (1991) 444-456.

F. De Geuser, A. Deschamps, *Precipitate characterisation in metallic systems by small-angle X-ray or neutron scattering,* C. R. Physique 13 (2012) 246–256.

A. Deschamps, *On the validity of simple precipitate size measurements by small-angle scattering in metallic systems,* J. Appl. Cryst. 44 (2011) 343–352.

E. Eidenberger et al., *Application of Photons and Neutrons for the Characterization and Development of Advanced Steels*, Adv. Eng. Mater. 13 (2011) 664-673.

SANS instrument under development in Delft